

Status of LHCb Upgrade-I and future prospects

CERN-RRB-2025-026

LHCb collaboration

29th April 2025

Contents

1	Introduction	4
2	Collaboration matters	6
3	Project organisation	6
4	Financial matters	7
5	Operations	8
6	Preparation of 2025 run	10
7	Physics	12
7.1	<i>CP</i> violation and the CKM matrix	13
7.2	Rare decays	15
7.3	Semileptonic <i>B</i> decays	16
7.4	Ions and Fixed target	16
7.5	Spectroscopy	18
8	Tracking detectors	18
8.1	Vertex Locator (VELO)	18
8.1.1	Work over YETS 2024/025	19
8.1.2	Operation and performance studies	20
8.1.3	SMOG2	21
8.2	Upstream Tracker (UT)	22
8.2.1	Introduction and overview	22
8.2.2	2024 Heavy Ion Run	23
8.2.3	YETS work	23
8.2.4	Progress in TELL40 firmware	24
8.3	Scintillating-Fibre Tracker (SciFi)	24
8.3.1	System overview	24
8.3.2	Detector operation and performances	25
8.3.3	Maintenance activities during YETS	27
9	Particle identification detectors	29
9.1	Cherenkov detectors (RICH)	29
9.1.1	System overview	29
9.1.2	Maintenance and YETS activities	29
9.1.3	Performance and readiness for data taking	31
9.2	Calorimeters (ECAL and HCAL)	32
9.2.1	System overview	32
9.2.2	Maintenance over YETS	32
9.2.3	Calibration	33

9.2.4	Reconstruction and monitoring	33
9.3	Muon chambers (MUON)	34
10	PLUME and luminosity	35
10.1	System overview	35
10.2	PLUME-based online luminosity	36
11	VELO-based online luminosity and beam-spot monitoring	37
11.1	Offline luminosity determination	40
12	Real time analysis	41
12.1	First trigger stage	41
12.2	Alignment and calibration	42
12.3	Second trigger stage	43
13	Online	44
14	Electronics	45
15	Software and computing	45
15.1	Data processing	45
15.2	Simulation	46
15.3	Offline computing	47
16	Infrastructure	48
17	Upgrade-II status	49

1 Introduction

The original LHCb detector completed data taking at the end of LHC Run-2 in 2018. The LHCb Upgrade I was primarily installed during LHC LS2 in 2018-2022, with the last subsystem, the Upstream Tracker (UT), finally installed later during the YETS 2022/23. A further detector upgrade, the LHCb Upgrade II, is planned to be installed in LS4, with some first enhancements of the present detector to be implemented already in LS3. Progress on the Upgrade-II design and scoping is also described in this document.

A total of 10fb^{-1} were delivered to LHCb in Run 1 and Run 2 data taking periods, with 9fb^{-1} recorded. The LHCb Run-1 and Run-2 dataset comprises pp , $p\text{Pb}$, and PbPb at various centre-of-mass energies, as well as pA ($A = \text{He, Ne, Ar}$) collisions in fixed target mode, using the experiment's unique gas injection system. Exploitation of Run 1 and Run 2 data is still progressing.

The LHCb Upgrade-I detector has been operated with design performances during 2024, after the successful recovery of the VELO detector in the YETS 2023/24, following an incident in the LHC vacuum system in the YETS 2022/23. The Upgrade-I detector is based on a novel trigger system able to read out all sub-detectors at 40 MHz and to select physics events of interest by means of a pure software trigger based on GPUs (first stage) and CPUs (second stage). The software trigger allows the experiment to collect data with high efficiency at a luminosity of up to $2 \times 10^{33} \text{cm}^{-2}\text{s}^{-1}$. Flavour-physics measurements are going to be performed with higher precision than was possible with the previous detector and across a wider range of observables. The flexibility inherent in the new trigger scheme will also allow the experiment to diversify even further its physics programme in important areas beyond flavour. During 2024, the Upgrade-I detector has been operated in nominal luminosity conditions, recording about 9.5fb^{-1} of integrated luminosity in proton-proton collisions, hence surpassing in a single year the combined integrated luminosity of LHC Run-1 and Run-2 (see Fig. 1). During the 2024 heavy-ion run, which was preceded by a proton-proton reference run, LHCb collected the largest integrated luminosity ever recorded by the experiment, larger than all previous runs combined. The corresponding luminosity plots are shown in Fig. 2.

The Upgrade I detector was proposed in the Letter of Intent [1] in 2011, and its main components and cost-envelope were defined in the Framework TDR [2] one year later. Technical Design Reports (TDRs) were written for all systems [3–11] and approved by the CERN Research Board. Addenda to the Memorandum of Understanding (MoU) were presented to the RRB in April and October 2014, covering the division of resources and responsibilities for Common Project items [12] and sub-system items [13], respectively. Enhancements to the ECAL and RICH systems are proposed for LS3 and were approved in December 2023. A TDR for additional enhancements to the Online system in LS3 was submitted to the LHCC in February 2024, and approved in September 2024.

The LHCb Upgrade II detector was proposed in the Expression of Interest [14]

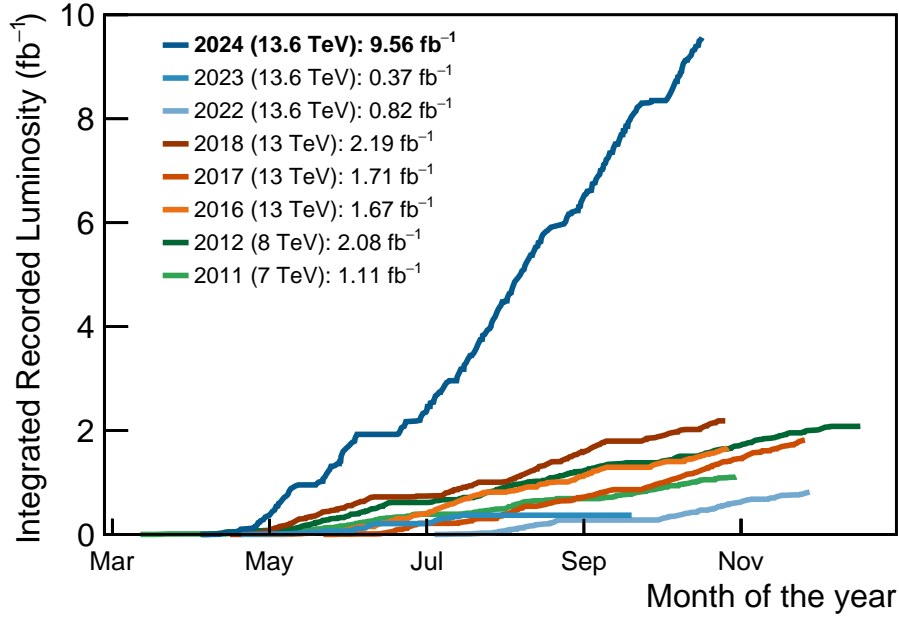


Figure 1: LHCb integrated luminosities for proton-proton collisions in the various LHC running years.

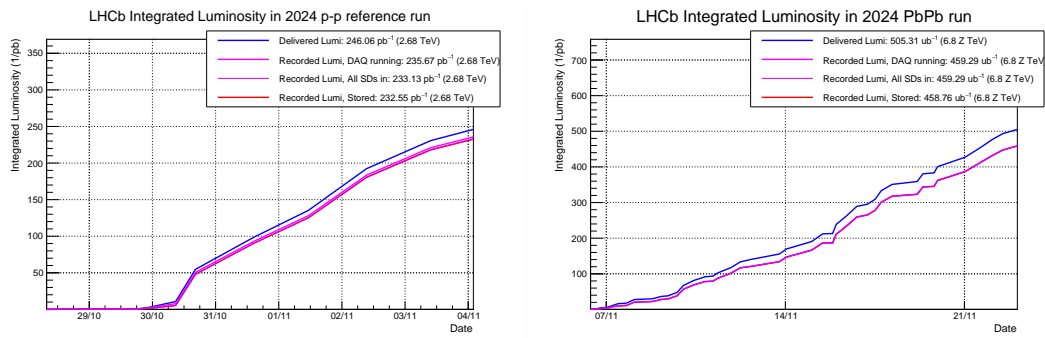


Figure 2: LHCb integrated luminosities of (left) the 2024 proton-proton reference run and (right) the 2024 heavy-ion run.

in 2017 and the Physics Case described in [15]. Its main components and cost-envelope were defined in the Framework TDR [16] that was approved in 2022. A Scoping Document, describing various scoping scenarios in terms of cost and physics performances, was submitted to the LHCC in September 2024, and its approval was recommended by the LHCC in March 2025, and soon after approved by the CERN Research Board.

2 Collaboration matters

Since last RRB meeting, six new institutions have joined LHCb, all of them as Technical Associate Members

- University of Science and Technology of China (USTC), associated through University of Chinese Academy of Sciences;
- Henan Normal University, associated through the Institute of Particle Physics, Central China Normal University;
- University of Leicester, associated through thr University of Warwick;
- Northwestern Polytechnic University, associated through IHEP Beijing;
- Laboratoire de Physique Corpusculaire de Caen, associated through IJCLab Orsay;
- INFN Trento Institute for Fundamental Physics and Applications (TIFPA), associated through INFN Cagliari.

3 Project organisation

The management of the experiment is composed of the Spokesperson and two deputies, the Technical Coordinator, the Resource Coordinator and the Software and Computing Coordinator.

The Upgrade I detector is overseen by the LHCb Technical Board. The Technical Board is chaired by the Technical Coordinator and is comprised of all detector project leaders. Day-by-day detector work is overseen by the technical coordination team. The commissioning and operations of the Upgrade I detector are overseen by the Run coordinator and discussed twice per week at Run meetings, with representatives from all projects. Physics aspects are overseen by the Physics Coordinator and discussed at the Physics Planning Group, whereas Operational aspects are overseen by the Operations Coordinator and discussed at the Operations Planning Group.

The Software and Computing Coordinator chairs the Software and Computing Board, which includes the project leaders of the software and computing projects, and the software coordinators of the various subdetectors.

During 2024, a subcommittee of the Technical Board (TBSC) was put in place to strengthen communication between the Real Time Analysis project, the Online project, and the subdetector projects to manage software tools and components of common interest. An additional deputy Technical Coordinator was appointed for a period of one year with the mandate to chair this subcommittee. As initially planned, the TBSC has been disbanded at the end of 2024.

Activities related to LHCb Upgrade-II are overseen by the Upgrade II Planning Group, chaired by the Upgrade-II Coordinator and composed of several members with specific responsibilities in the various areas of physics performance, hardware and software development.

4 Financial matters

After having been constant for a long time, in 2024 the RRB agreed, upon recommendation by the Scrutiny Group, to increase the M&O A budget to 3,120 kCHF. The increase of 50 kCHF was necessary to compensate for the rapidly increasing costs of various service-level agreements (SLAs) with technical services at CERN.

Throughout the year, the entire detector has operated at high efficiency. Important consolidation work was done in the Online systems and also in the technical infrastructure for various sub-detectors. There is still a worrying trend in rising SLA costs and important expenditures will be needed during LS3 to replace very old parts of the Online as well as the Technical infrastructure. These issues will be discussed in detail with the Scrutiny Group and their advice will be sought to prepare a comprehensive plan through LS3.

Following the resolution of the CERN council to terminate the International Collaboration Agreement with Russia, Russian institutes are no longer participating to the LHCb collaboration since the end of November 2024. Following the advice of the RRB and the Director of Research and Computing, 11/12ths of the due amount for M&O A and B have been invoiced to Russia, but only received to a small extent so far. The accumulated outstanding contributions of 378 kCHF from Russia (combining M&O-A and B) remain on the books.

Besides open invoices, Russian contributions to M&O A and B will no longer be available by the beginning of 2025. The remaining funding agencies have agreed to accept to increase their contributions to cover the shortfall due to the missing Russian contributions from 2025 onward (CERN-RRB-2024-099), which amounts to an increase of approximately 9.8 per cent, for which the LHCb collaboration is very grateful.

The financial requirements for the construction of the LHCb Upgrade I were defined in detail in Addendum No. 1 to the Memorandum of Understanding (MoU) for Common Projects [12] and in Addendum No. 2 for the sub-detector systems [13], which refer to the Framework Technical Design Report [2] and the Technical Design Reports [3–8] for all subdetectors.

The Upgrade I construction has been completed within the agreed cost enve-

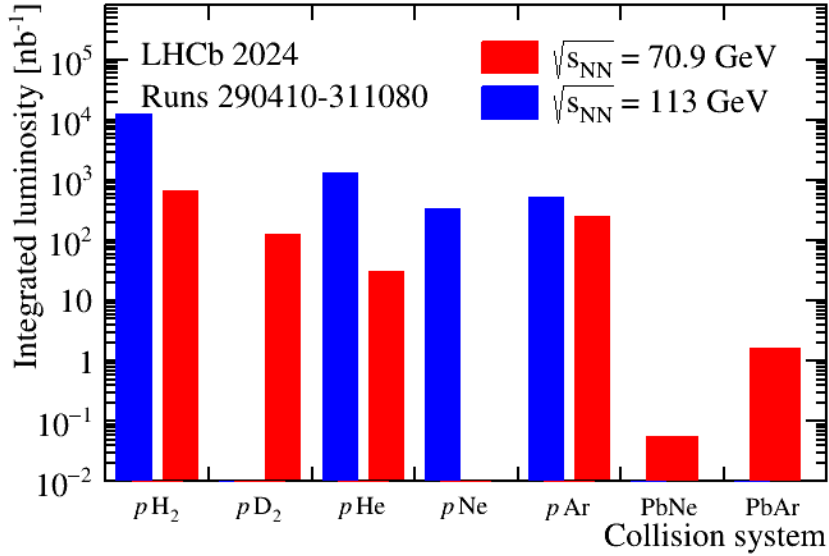


Figure 3: Integrated luminosities for different fixed-target collisions at LHCb in 2024.

lope. At the end of 2024 the books and accounts were closed as decided by the RRB in the October 2023 session. We will therefore not report on them any longer.

5 Operations

After a successful proton-proton campaign, the 2024 data taking ended with the Heavy Ion programme including a proton-proton reference run. Lead-lead collisions were recorded with minimum bias triggers and in parallel the SMOG2 storage cell was used to record fixed-target lead-neon and lead-argon collisions. During the proton-proton reference run hydrogen, deuterium, helium and argon were injected. The integrated luminosities are given in Fig. 3. All data have been processed offline and are available for data analysis. Further information on the recorded luminosities of proton-proton and lead-lead collisions is given in Sec. 7.

The offline data quality team, using inputs from online monitoring and the full event reconstruction in HLT2, characterises the data as suitable (good) or not (bad) for physics analyses. Another category (conditional) for data which are potentially useful for some or all analyses but exhibit features which need to be corrected has been introduced in the last months. One example where this category is used is a fill during the lead-lead run in which the LHC was transmitting the wrong filling scheme. This needs to be corrected in the analysis of SMOG data to correctly assign the collision type (beam-beam or beam-empty). The new category is also used for the nominal proton-proton data in some cases, and analysts can use it to slightly increase the total statistics.

During nominal proton-proton running the data are split into 3 main streams

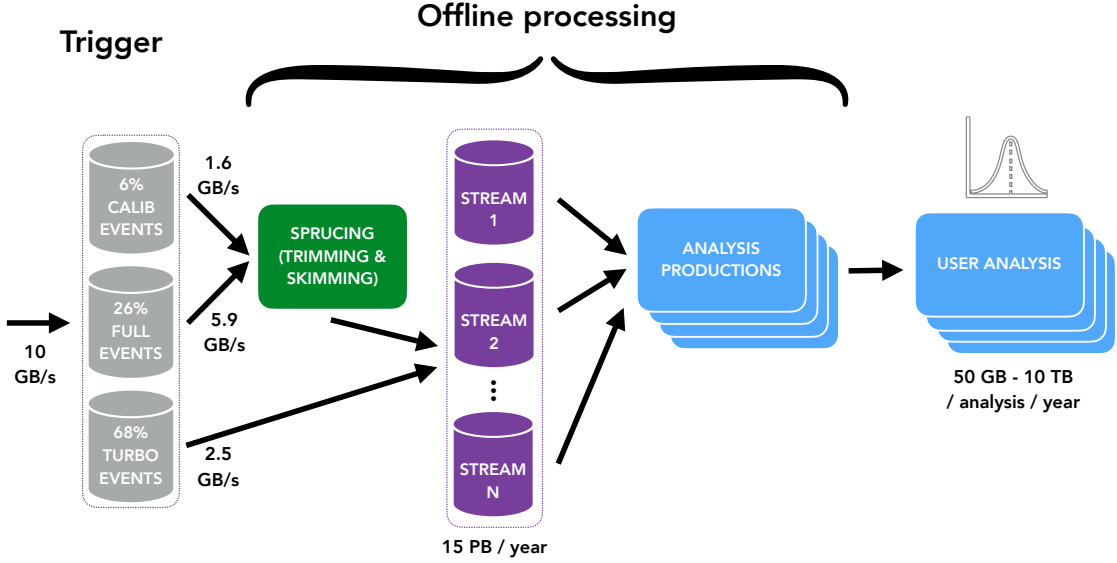


Figure 4: Schematic view of the offline processing for the LHCb Upgrade-I.

after the trigger and before offline processing, as shown in Fig. 4. In the offline processing, the Calib and Full events undergo the so-called Sprucing which allows further selections to be applied, reducing the amount of data stored on disk and available to analysts. The Turbo stream is only split into smaller streams, with each stream representing one physics working group, but no additional selections or data reduction are performed. As foreseen by the LHCb Computing Model [17], the Full stream data of 2024 was reprocessed in the last YETS to allow for a retuning of existing event selections and the addition of new ones. The reprocessing was performed as planned and is now over. For 2025, the streaming of the Turbo stream was reviewed, reducing the amount of duplicated information when splitting into smaller streams. This also allows more and smaller streams to be created, reducing significantly the bandwidth required for user jobs (so-called Analysis Productions). As this development could also reduce the data size of 2024 Turbo data by 30%, the Operations Planning Group decided to perform this unplanned processing on short notice, supported by CERN IT. More details on the offline processing of the data can be found in Sec 15.

The Luminosity Working group has provided the first (offline) calibration of the luminosity which can be used by analysts to determine the integrated luminosity of their dataset, indicating small corrections to be applied to the luminosity determined online during detector operation. For 2025, this difference will be also corrected.

The process of validating and tuning the description of the sub-detectors, trigger and offline selections in the simulation framework is actively ongoing. Simulations with improved detector description were made available throughout the year. As the data taking conditions changed throughout 2024, options for different trigger and reconstruction configurations have been provided. Differences between

data and simulation have been studied by several analyses and have been presented during the so-called Analysis and Software week at beginning of February 2025. Recently, a new simulation version with updated event generators has been released. In addition, samples with known changes in the detector geometry (see, *e.g.*, the discussion on the VELO shims later in this document) were produced to allow a preliminary study of reconstruction software and selections in HLT1. Another update of the simulation is currently being validated and expected to be released very soon. This update significantly improves the description of the detector response for most sub-detectors.

One of the operational goals for 2025 is to achieve more stable conditions throughout the year to ease data analysis. In order to achieve this, the members of the Operations Planning Group (OPG) have established a plan for the activities during the shutdown and throughout the year, including a software release schedule. One of the planned updates is an improved description of the magnetic field map, used in the reconstruction software and simulation. The measurement campaign has been organised by the Technical Coordination and the integration is being followed by the OPG. Figures of merit, based on 2024 data, to assess the improvements have been defined and will allow quick validation with early 2025 data to take a decision before physics production starts. The other focus has been a review and tuning of physics selection in HLT1, HLT2 and Sprucing. The output bandwidth, measured in 2024 when reaching nominal luminosity in the last two weeks of the proton-proton run, would not be sustainable for an entire data-taking year without exhausting storage resources available on the WLCG grid, taking into account that the LHC will also provide a higher number of bunches to LHCb in 2025. Bandwidth targets including safety margins have been defined by the Offline Computing team. Together with the Real Time Analysis and Data Processing and Analysis projects, the Physics Working Groups are working towards meeting these targets.

6 Preparation of 2025 run

Thanks to the commitment of the expert teams, piquets, shifters and run coordination during 2024, a record amount of integrated luminosity was collected, corresponding to more than 9 fb^{-1} of 6.8 TeV pp collisions, 0.23 fb^{-1} pp reference data at an energy of 2.68 TeV, together with 0.45 nb^{-1} of 6.8 Z TeV PbPb collisions. Towards the end of data taking, efficiencies of more than 95% at nominal pileup conditions were routinely achieved. The experiment operated the SMOG2 programme in parallel, injecting He, Ne, Ar, H₂ and D₂ for a wide range of fixed-target data taking, as summarised in Fig. 3. At the end of the year, an in-depth debriefing campaign was launched, in order to identify any factors which could contribute to gaining the last few percent of performance and improve the quality, stability and efficiency of data taking in 2025.

Concerning the subdetector performance, the YETS was fully exploited to

address remaining hardware sources of inefficiency, a few highlights of which are mentioned here. 2024 saw the loss of three fills due to magnet trips during adverse environmental conditions in the summer, for which mitigations have been put in place (see Sec.). The issue of VTRx link outgassing, which affects experiments CERN-wide, resulted in the loss or degraded performance of some control and data links during the year. LHCb is able to open the experiment and access a large fraction of these links, and hence could carry out an extensive campaign of fibre cleaning during the YETS, in particular for SciFi and RICH. This results in the recovery of the affected links as well as prolonging the time expected for good performance for the remaining links. The PLUME detector has implemented new LED monitoring to allow gain calibration with LEDs in 2025, in addition with a system to measure the beam-phase shift with respect to the LHC clock, as part of a significantly enhanced 40 MHz monitoring system. The SMOG2 system has been upgraded with high-pressure gas reservoirs, with 200 bar pressure as compared to the previously available 1.5 bar. This will smooth operations, allowing a faster and more constant preparation time per fill. The controls have also been enhanced to allow three coarse pressure set points per gas with fine tuning also possible, allowing a quick reaction to data-taking conditions. In 2024 the inefficiency due to DAQ dead time was on average less than 1% per fill, however in certain circumstances, it could reach up to 7%. The effect was studied over the YETS and a solution put in place to reduce the root cause. The PLUME detector has installed new firmware to allow LED monitoring and readout which will allow gain calibration in 2025 with LEDs as well as enhanced monitoring, and a measurement of the beam-phase shift with respect to the LHC clock. This will add redundancy and robustness to the online luminosity provision. The sources of data-taking inefficiency are multiple and can often be interlinked, so for instance a loss of efficiency due to the time needed to close the VELO per fill can be exacerbated by a dead time in the DAQ, and the global improvement in performance across the subsystems is expected to enhance the data taking for 2025. The monitoring framework is being constantly refreshed in order to make optimum use of the shifter effort in the control room to follow the evolution of the detector reliability, fine tuning the reference histograms and methods of storing and communicating any detector performance evolution through the year.

The LHC will work towards a target of 1.8×10^{11} protons per bunch in 2025, taking advantage of the available margin on the cryogenic heat loads in the machine identified during the 2024 run. The decision of the directorate is to favour a scheme running up to the end of the summer with 1.8×10^{11} protons per bunch and then to gradually increase the intensity from the start of September to reach the target.

In general, 36 bunch train BCMS filling schemes are favoured, which give a simpler operation. The target for the start up is to reach $4 \times 36b$ operation, which is a compromise between the safe cryo limit and will still give more collisions in LHCb than last year (2227 as compared to the previous 2133) and more bunches total (2460 as compared to the previous 2352) which enhances the luminosity for SMOG2. The top priority of the experiment is to accumulate a large pp dataset

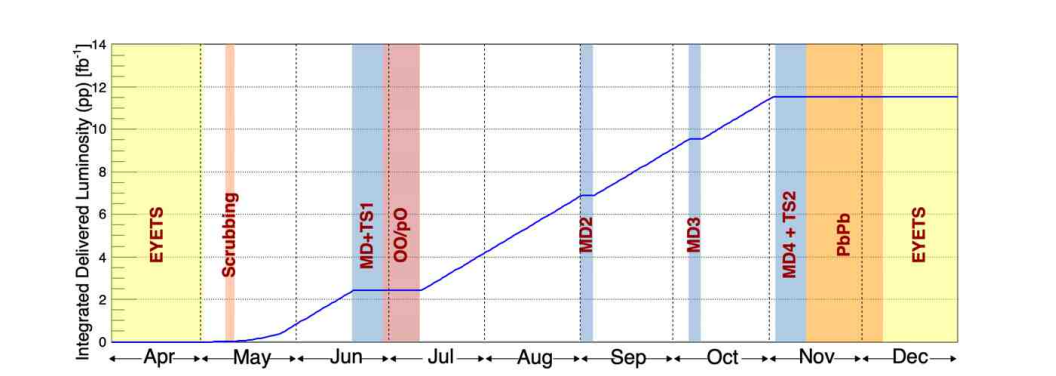


Figure 5: Expectation for LHC schedule 2025

in the most stable operational conditions possible. The anticipated integrated delivered luminosity and the planning of the year is shown in Fig. 5.

In July there are approximately 8 days allocated for special runs, in which the LHC will circulate and collide oxygen beams at 5.36 Z TeV, and provide both p -O and O-O collisions, followed by a day of operation devoted to Neon-Neon collisions. LHCb is eagerly awaiting these data and expects to benefit from its unique high rapidity reach and the enhanced granularity of the upgraded detector, allowing full centrality to be reached. The LHC scenarios include a squeeze to a β^* of 1 m for LHCb, with zero crossing angle. The delivered luminosity targets are 0.5 nb^{-1} for O-O and 2 nb^{-1} for p -O. The special running period will be followed by a van der Meer programme for all experiments for which LHCb plans a full programme of scans, with enhancements where possible such as a de-squeezed beam to enhance the beam-gas imaging measurement and a continuous scan, which will be performed for the first time at the LHC. LHCb looks forward to the PbPb data taking at the end of the year, during which we expect to benefit from enhanced levelling times, if the newly commissioned $\beta^* = 1 \text{ m}$ commissioning is successful, on top of the 40% increase in number of colliding bunches provided by the LHC and the operations with magnet up polarity, which reduces the effective crossing angle.

7 Physics

From October 2024 to April 2025 the LHCb collaboration submitted 27 new physics publications. This brings the number of submitted LHCb physics publications to a total of 768 at the time of writing (not including a dozen of collaboration papers on physics performances), of which 745 are already published. Further 21 publications are being processed by the LHCb Editorial Board and are close to submission. All submitted papers relative to this period are listed in Table 1. In the following, selected results from recent publications are briefly highlighted.

Table 1: Full list of LHCb results submitted for publication from November 2024 to April 2025.

	Title	arXiv	Ref.
1.	Test of lepton flavour universality with $B_s^0 \rightarrow \phi \ell^+ \ell^-$ decays	2410.13748	[18]
2.	Measurements of $\psi(2S)$ and $\chi_{c1}(3872)$ production within fully reconstructed jets	2410.18018	[19]
3.	Measurement of the CKM angle γ in $B^\pm \rightarrow DK^*(892)^\pm$ decays	2410.21115	[20]
4.	Study of $D_{s1}(2460)^+ \rightarrow D_s^+ \pi^+ \pi^-$ in $B \rightarrow \bar{D}^{(*)} D_s^+ \pi^+ \pi^-$ decays	2411.03399	[21]
5.	Measurement of $\psi(2S)$ to J/ψ cross-section ratio as a function of centrality in PbPb collisions at $\sqrt{s_{NN}} = 5.02$ TeV	2411.05669	[22]
6.	Constraints on the photon polarisation in $b \rightarrow s \gamma$ transitions using $B_s^0 \rightarrow \phi e^+ e^-$ decays	2411.10219	[23]
7.	Measurement of ϕ meson production in fixed-target p Ne collisions at $\sqrt{s_{NN}} = 68.5$ GeV at LHCb	2411.09343	[24]
8.	First evidence for direct CP violation in beauty to charmonium decays	2411.12178	[25]
9.	Study of Λ_b^0 and Ξ_b^0 decays to $\Lambda h^+ h'^-$ and evidence for CP violation in $\Lambda_b^0 \rightarrow \Lambda K^+ K^-$	2411.15441	[26]
10.	Observation of the open-charm tetraquark state $T_{cs0}^*(2870)^0$ in the $B^- \rightarrow D^- D^0 K_S^0$ decay	2411.19781	[27]
11.	Search for D^0 meson decays to $\pi^+ \pi^- e^+ e^-$ and $K^+ K^- e^+ e^-$ final states	2412.09414	[28]
12.	Test of lepton flavour universality with $B^+ \rightarrow K^+ \pi^+ \pi^- \ell^+ \ell^-$ decays	2412.11645	[29]
13.	Measurement of CP asymmetries in $\Lambda_b^0 \rightarrow p h^-$ decays	2412.13958	[30]
14.	Measurement of CP asymmetry in $B_s^0 \rightarrow D_s^\mp K^\pm$ decays	2412.14074	[31]
15.	Study of light-meson resonances decaying to $K_S^0 K \pi$ in the $B \rightarrow (K_S^0 K \pi) K$ channels	2501.06483	[32]
16.	Search for charge-parity violation in semileptonically tagged $D^0 \rightarrow K^+ \pi^-$ decays	2501.11635	[33]
17.	Observation of the $\Lambda_b^0 \rightarrow J/\psi \Xi^- K^+$ and $\Xi_b^0 \rightarrow J/\psi \Xi^- \pi^+$ decays	2501.12779	[34]
18.	Evidence for the $B^- \rightarrow D^{*0} \tau^- \bar{\nu}_\tau$ decay	2501.14943	[35]
19.	Measurement of the multiplicity dependence of Υ production ratios in pp collisions at $\sqrt{s} = 13$ TeV	2501.12611	[36]
20.	Search for resonance-enhanced CP and angular asymmetries in the $\Lambda_c^+ \rightarrow p \mu^+ \mu^-$ decay at LHCb	2502.04013	[37]
21.	Angular analysis of $B^0 \rightarrow K^{*0} e^+ e^-$ decays	2502.10291	[38]
22.	Observation of a new charmed baryon decaying to $\Xi_c^+ \pi^+ \pi^-$	2502.18987	[39]
23.	Branching fraction measurement of the decay $B^+ \rightarrow \psi(2S) \phi(1020) K^+$	2503.02711	[40]
24.	Observation of charge-parity symmetry breaking in baryon decays	2503.16954	[41]
25.	Observation of the doubly-charmed-baryon decay $\Xi_{cc}^{++} \rightarrow \Xi_c^0 \pi^+ \pi^+$	2504.05063	[42]
26.	Observation of the very rare $\Sigma^+ \rightarrow p \mu^+ \mu^-$ decay	2504.06096	[43]
27.	Angular analysis of the decay $B_s^0 \rightarrow \phi e^+ e^-$	2504.06346	[44]

7.1 CP violation and the CKM matrix

Over the last six months, the LHCb collaboration has been very prolific and successful in providing new experimental results in the area of CP violation. A long awaited result concerns the first observation of charge-parity symmetry breaking in baryon decays [41]. This was achieved using the full dataset available from Run-1 and Run-2 to perform the $\Lambda_b^0 \rightarrow p K^- \pi^+ \pi^-$ yield asymmetry measurement in various regions of phase-space. The $\Lambda_b^0 \rightarrow \Lambda_c^+ (\rightarrow p K^- \pi^+) \pi^-$ control mode, producing the same visible final state via a charm resonance, is used to measure corrections from differences in production and detection effects. These are found to be at the 1% level, while the phase-space integrated asymmetry measurement in the signal channel yields $(2.45 \pm 0.46 \pm 0.10)\%$. This constitutes a 5.3σ observation of CP

violation effects in b -baryon decays to four body final states. Further studies were carried out by analysing local asymmetries, where the choice of the phase-space region is motivated by the presence of well-known hadronic resonances. Other recent results on CP violation in baryonic decay modes concern the measurement of asymmetries in $\Lambda_b \rightarrow ph^-$ decays with Run-2 data, where $h \equiv \pi, K$ [30]. When combining with the Run-1 results, this baryonic decay to two final state particles yields $\mathcal{A}_{CP}^{pK^-} = (-1.1 \pm 0.7 \pm 0.4)\%$ and $\mathcal{A}_{CP}^{p\pi^-} = (0.2 \pm 0.8 \pm 0.4)\%$, constituting the most precise measurements of these asymmetries to date, although both of them are compatible with the CP conservation hypothesis. Studies of three-body decays of Λ_b^0 and Ξ_b^0 baryons were also tackled, in particular, analysing the Λhh final state, and are reported in Ref. [26]. The corresponding branching-fraction measurements of $\Lambda_b^0/\Xi_b^0 \rightarrow \Lambda h^+ h'^-$ decays are more precise than and supersede previous LHCb results [45]. The CP asymmetries are measured for $\Lambda_b^0 \rightarrow \Lambda h^+ h'^-$ and $\Xi_b^0 \rightarrow \Lambda K^- \pi^+$ decays, with respect to the $\Lambda_b^0 \rightarrow \Lambda_c^+(\rightarrow \Lambda \pi^+) \pi^-$ decay. Evidence for CP violation is found in the $\Lambda_b^0 \rightarrow \Lambda K^+ K^-$ decay for the first time, with $\Delta A_{CP} = (8.3 \pm 2.8)\%$ integrated over the final-state phase space. The CP asymmetry is enhanced in the N^{*+} mass region, where it is measured to be $\Delta A_{CP} = (16.5 \pm 5.1)\%$. No evidence of CP violation is found for the other Λ_b^0/Ξ_b^0 decays that are studied.

A new measurement of the CP -asymmetry difference between $B^+ \rightarrow J/\psi h^+$ decay modes, $\Delta A_{CP} \equiv \mathcal{A}_{CP}(B^+ \rightarrow J/\psi \pi^+) - \mathcal{A}_{CP}(B^+ \rightarrow J/\psi K^+)$ [25] has been measured to show a 3.2σ deviation from zero, providing first evidence for direct CP violation in beauty decays to charmonium final states. This effect can be attributed to the enhanced penguin-to-tree ratio in $B^+ \rightarrow J/\psi \pi^+$ decays compared to that in golden $b \rightarrow c\bar{c}s$ transitions. Both ΔA_{CP} and the ratio of branching ratio measurements serve to control the effects of the penguin contributions affecting the determination of the CP -violating phase 2β in the golden channel $B^0 \rightarrow J/\psi K^0$, using approximate SU(3) flavour symmetry.

Regarding the study of CP -violating effects in the charm sector, an analysis of the flavour oscillations of the charmed neutral meson is presented in Ref. [33]. The ratio of the doubly Cabibbo-suppressed $D^0 \rightarrow K^+ \pi^-$ to the Cabibbo-favoured $D^0 \rightarrow K^- \pi^+$ decay rates is measured as a function of the decay time of the D^0 meson and compared with the charge-conjugated system to search for charge-parity violation. In this analysis, the charm mesons are selected as originating from the decays of B mesons, ensuring a significant displacement from the pp interaction point, thus providing a clean access to the shortest decay times. The flavour oscillation parameters, relating to the differences in mass and width of the mass eigenstates, are found to be $y' = (5.8 \pm 1.6) \times 10^{-3}$ and $(x')^2 = (0.0 \pm 1.2) \times 10^{-4}$. No evidence for charge-parity violation is seen either in the flavour oscillations or in the decay, where the direct charge-parity asymmetry is measured to be $A_D = (2.3 \pm 1.7)\%$.

Two new determinations of the CKM angle γ are obtained from measurements of CP asymmetries in $B_s^0 \rightarrow D_s^\mp K^\pm$ decays [31], providing the most precise determination of γ in the B_s^0 system, and in $B^\pm \rightarrow DK^*(892)^\pm$ decays

[20]. The later analysis presents the simultaneous measurement of γ with 2-, 3- and 4-body $D^0(\bar{D}^0)$ decays and achieves, making use of the full Run 1 and Run 2 data sample, the first observation of the Doubly-Cabibbo-Suppressed (DCS) $B^\pm \rightarrow [\pi^\pm K^\mp]_D K^{*\pm}$ and $B^\pm \rightarrow [\pi^\pm K^\mp \pi^\pm \pi^\mp]_D K^{*\pm}$ decays. The CP fit to 2- and 4-body D decays, and for the first time at LHCb to 3-body decays with Dalitz input from CLEO3 and BESIII, yields $\gamma = (63 \pm 13)^\circ$. Upon combination with other LHCb results, the uncertainty on γ is brought below the $\pm 3^\circ$ target for the end of Run-2: $\gamma = (64.6 \pm 2.8)^\circ$ [46].

7.2 Rare decays

The collaboration has conducted two new tests of lepton-flavour universality (LFU) tests in rare B -meson decays, specifically analysing the $B_s^0 \rightarrow \phi \ell^+ \ell^-$ and the $B^+ \rightarrow K^+ \pi^- \pi^+ \ell^+ \ell^-$ decay modes [18,29]. These studies compare the branching fractions of decays involving electrons and muons in different regions of the invariant mass squared of the lepton pair (q^2) to probe potential LFU violation. The measured ratios are compatible with the Standard Model expectations. The results reported in Ref. [18] constitute the first LFU ratio measured in the B_s^0 system, and, together with the results of Ref. [23], provide the first observation of the $B_s^0 \rightarrow \phi e^+ e^-$ decay mode. This last result studied the branching ratio of the $B_s^0 \rightarrow \phi e^+ e^-$ decay mode in the very low q^2 region, $0.0009 < q^2 < 0.2615 \text{ GeV}^2/c^4$, where the dominant contribution to the decay rate arises from the influence of the photon pole and has sensitivity to form factors and the value of the $C_7^{(\prime)}$ Wilson coefficients, which in turn are sensitive to right-handed currents. In addition to these, angular analyses of the $B_s^0 \rightarrow \phi e^+ e^-$ and the $B^0 \rightarrow K^{*0} e^+ e^-$ decays using the full Run 1 and 2 data are reported in Refs. [44] and [38], respectively. The comparison of these results with the corresponding ones from the muonic modes allow for a LFU comparison of the angular coefficients that describe the multi-dimensional decay rate. The measured observables are broadly in agreement with the Standard Model predictions, with the largest differences of around 2σ found for F_L and A_{FB} in the $B^0 \rightarrow K^{*0} e^+ e^-$ decay mode. Overall, no significant deviations from the Standard Model expectations are seen with these decays.

Other recent results in rare decays involve charm and strange processes. A search for D^0 meson decays to $\pi^+ \pi^- e^+ e^-$ and $K^+ K^- e^+ e^-$ final states [28] was conducted with Run-2 data. The decay $D^0 \rightarrow \pi^+ \pi^- e^+ e^-$ is observed for the first time when requiring that the two electrons are consistent with coming from the decay of a ϕ or ρ/ω mesons. No evidence is found for the $D^0 \rightarrow K^+ K^- e^+ e^-$ decay and world-best limits are set on its branching fraction, which improves previous best limits by two orders of magnitude. The results are compared to, and found to be consistent with, the branching fractions of the $D^0 \rightarrow \pi^+ \pi^- \mu^+ \mu^-$ and $D^0 \rightarrow K^+ K^- \mu^+ \mu^-$ decays recently measured by LHCb, and confirm lepton universality at the current level of precision. Another result in rare charm decays pertains the search for resonance-enhanced CP and angular asymmetries in the $\Lambda_c^+ \rightarrow p \mu^+ \mu^-$ decay process with Run 2 data [37]. The total decay width in this

process is dominated by the intermediate $\Lambda_c^+ \rightarrow p\phi$ resonant decay and therefore the measurement of the asymmetries is performed in two dimuon invariant mass regions near the ϕ -meson mass, on account of the limited statistics available for this rare decay mode. The results confirm the Standard Model prediction of no-asymmetry with the current available precision. In the rare and strange sector, the observation of the $\Sigma^+ \rightarrow p\mu^+\mu^-$ decay, together with its branching fraction measurement and the study of the di-muon invariant mass spectrum in this decay mode are reported in Ref. [43]. No evidence of resonant structures is found in the di-muon invariant-mass distribution, in agreement with the Standard Model expectation for a phase-space like distribution. This represents the rarest baryon decay ever observed.

7.3 Semileptonic B decays

Evidence for the $B^- \rightarrow D^{**0}\tau^-\bar{\nu}_\tau$ decay mode, at the 3.5σ level, has been reported in Ref. [35] using data collected by LHCb during the Run-1 and Run-2 data-taking periods. The D^{**0} symbol is used here to represent any of the three excited charm mesons $D_1(2420)^0$, $D_2^*(2460)^0$, and $D_1'(2400)^0$. Currently, a significant source of systematic uncertainty common to all $\mathcal{R}(D^{(*)})$ measurements arises from the poorly known contribution from the so-called feed-down backgrounds, originating from these excited charm resonances. The branching ratio measurement of the $B^- \rightarrow D^{**0}\tau^-\bar{\nu}_\tau$ decay mode reported in Ref [35] can be used to improve the control on the aforementioned feed-down backgrounds in the $\mathcal{R}(D^{(*)})$ measurements. In addition, with the use of external input for the branching fraction of the doubly charmed normalisation mode, the $\mathcal{B}(B^- \rightarrow D_{1,2}^{**0}\tau^-\bar{\nu}_\tau) \times \mathcal{B}(D_{1,2}^{**0} \rightarrow D^{*+}\pi^-) = (0.051 \pm 0.013(\text{stat}) \pm 0.006(\text{syst}) \pm 0.009(\text{ext})) \%$ branching fraction is determined, which in turn allows to obtain $\mathcal{R}(D_{1,2}^{**0}) = 0.13 \pm 0.03(\text{stat}) \pm 0.01(\text{syst}) \pm 0.02(\text{ext})$ for the LFU ratio by comparing with the branching fraction of the corresponding muonic decay mode. This result is compatible with the Standard Model prediction and with the assumptions made on the $\mathcal{R}(D^{(*)})$ measurements on the $\mathcal{R}(D^{**})$ value.

7.4 Ions and Fixed target

The production of charmonia, in particular of the J/ψ and $\Psi(2S)$ states, has long been considered a key probe for understanding the properties of the quark-gluon plasma (QGP), particularly, the interplay between cold and hot nuclear matter effects. The relative production of $\Psi(2S)$ to J/ψ states, both decaying to two muons, is studied in Ref. [22] as a function of centrality using the 2018 PbPb collision data collected at a nucleon-nucleon centre-of-mass energy of $\sqrt{s_{NN}} = 5.02$ TeV, corresponding to an integrated luminosity of around $230 \mu\text{b}^{-1}$. No significant dependence on the centrality is found with the current level of precision. A different study reported in Ref. [36] probes temperature effects in the QGP by measuring the relative rates of heavy-flavour quarkonia production. Due to Debye

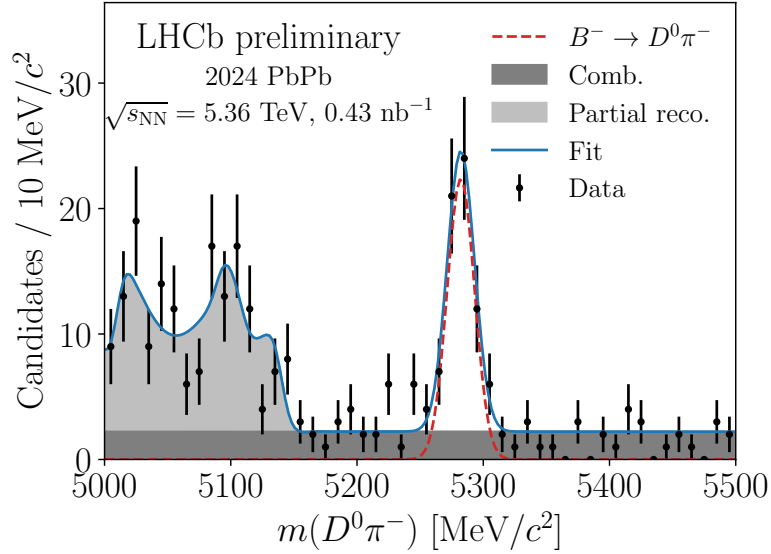


Figure 6: Heavy flavour signal from the 2024 PbPb run from LHCb-FIGURE-2025-004.

colour screening, surrounding partons prevent heavy quarks from combining into quarkonia, thus a significant suppression effect is expected for the $\Upsilon(3S)$ compared to the $\Upsilon(2S)$. The production ratios of $\Upsilon(3S)$ and $\Upsilon(2S)$ to $\Upsilon(1S)$ are measured as functions of different multiplicity variables in bins of (p_T, y) . A decreasing trend is observed for the normalised $\Upsilon(3S)/\Upsilon(1S)$ and $\Upsilon(2S)/\Upsilon(1S)$ ratios. The $\Upsilon(3S)$ state is found to be more suppressed, in line with other observations in larger collision systems and with the phenomenological predictions. A study aiming at Cold Nuclear Matter effects from QGP formation in small systems is reported in Ref. [24]. The enhancement of strange-hadron production as a result of the chemical equilibrium of strange quarks is one of the signatures of QGP formation. This effect is probed by measuring the $\phi(1020)$ meson production in fixed-target pNe collisions at $\sqrt{s_{NN}} = 68.5$ GeV. The differential cross-section is compared to predictions based on Pythia 8.312 and preliminary EPOS4 generators, which are found to generally underestimate the experimental points.

While detailed physics publications are not yet available, preliminary results from the 2024 PbPb run look extremely encouraging, with the LHCb detector to cover the centrality range 30–100%. With an integrated luminosity of about 0.45 nb^{-1} , several heavy-flavour meson and baryon decays are observed, some for the first time. An example is shown in Fig. 6, with the first observation of the $B^- \rightarrow D^0 \pi^-$ decay in PbPb collisions.

7.5 Spectroscopy

The study of both conventional and exotic spectroscopy states has resulted in several publications in the last months. An amplitude analysis to study the structure of $D_{s1}(2460)^+ \rightarrow D_s^+ \pi^+ \pi^-$ in $B \rightarrow \overline{D}^{(*)} D_s^+ \pi^+ \pi^-$ decays [21] finds a clear double-peak structure in the $m(\pi^+ \pi^-)$ spectrum which can be attributed to conventional light-flavoured states only if unpalatable large amplitudes are accepted. An alternative model with a new exotic $T_{c\bar{s}}^{++}$ state and its isospin partner $T_{c\bar{s}}^0$ is introduced and allows to describe the data. The $T_{c\bar{s}}$ mass and width are determined to be $2327 \pm 13 \pm 13$ MeV and $96 \pm 16 \pm 170$ MeV, where the first uncertainties are statistical and the second are systematic. Another amplitude analysis of the $B^- \rightarrow D^- D^0 K_S^0$ decay mode, using the full Run 1 and Run 2 LHCb data samples, reports the observation of a resonant structure with spin-parity 0^+ [27]. The measured mass and width of this structure, together with its quark content are consistent with those of the open-charm tetraquark candidate, $T_{c\bar{s}0}^*(2870)^0$, confirming the production of this state in a different decay mode than where it was previously observed. Further results on observations of new decay modes and production bounds on exotic states are reported in Refs. [34] and [40].

The study of conventional spectroscopy states has unveiled several new results, particularly in, but not limited to, the charm sector. The results shown in Ref. [39] report the observation of a new charmed baryon decaying to the $\Xi_c^+ \pi^+ \pi^-$ final state. Data from the Run 2 data-taking period are analysed to observe four states with high significance, including the discovery of the $\Xi_c(2923)^+$ baryon, and the first observation of the $\Xi_c(3080)^+$ baryon in this final state. Masses and widths are measured for all four states, and are competitive with, or more precise than, the existing world averages. The observation of the doubly-charmed-baryon decay $\Xi_{cc}^{++} \rightarrow \Xi_c^0 \pi^+ \pi^+$ is reported in Ref. [42], being only the fourth decay mode of this doubly-charmed baryon to be observed experimentally, despite the many more modes expected from theoretical predictions. This measurement provides important information towards an improved understanding of the decays of doubly charmed baryons, and contributes to shed light on the dynamics of low-energy interactions between two confined heavy quarks. An exhaustive study of light-meson resonances is presented in Ref. [32]. This work presents the first measurements of branching fractions for exclusive $B^+ \rightarrow R^0 K^+$ decays, where R^0 is an $I = 0$ resonance having $u\bar{u}$, $s\bar{s}$ or, possibly, gg content.

8 Tracking detectors

8.1 Vertex Locator (VELO)

The VELO in Upgrade-I is a pixel detector consisting of 52 modules, each equipped with four hybrid planar pixel tiles, arranged in thin walled radio-frequency (RF) boxes which form secondary vacuum enclosures within the LHC primary vacuum. It is cooled with evaporative CO₂ and provides a data-push triggerless readout,

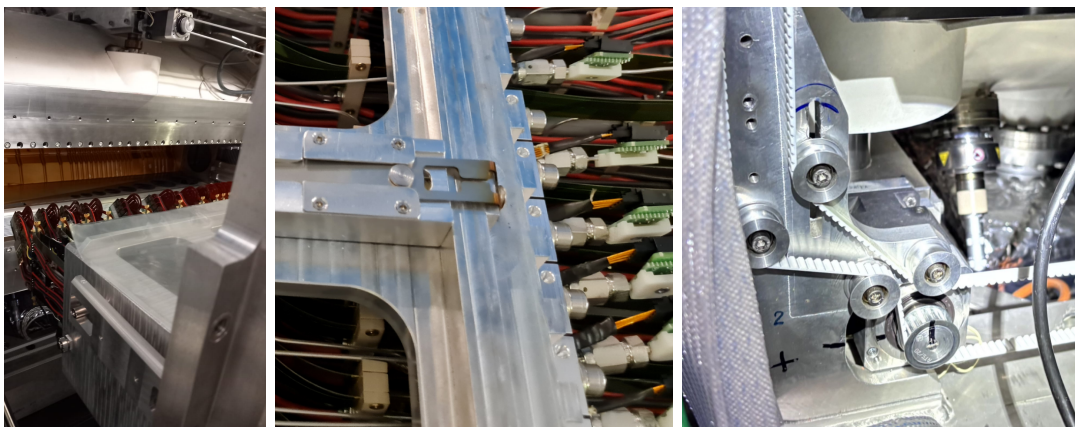


Figure 7: Left: The A-side retracted to repair the secondary vacuum seal. Middle: a view of the copper shims before the detector is inserted in the RF boxes. It is then retracted with a specialised tool. Right: the tensioning system of the VELO motion belt in its nominal position at the end of the YETS.

with the total rate reaching 1.2 Tb/s.

8.1.1 Work over YETS 2024/025

In the 2023/24 YETS, the RF box was replaced in a 16 weeks intervention. While the main repair was successful, a leak in the detector volume was found in the last days of the work programme. While not critical in terms of safety nor for operation, it prevented to perform any cycle of venting and pumping back of the detector (and of the LHCb beam pipe), as it was not possible to guarantee that the leak would remain stable after a change of mechanical load. This was in turn preventing to remove the shims that were keeping the detector slightly retracted from its nominal position during a technical stop in 2024. This was fixed in an intervention at the beginning of 2025, illustrated in the pictures of Fig. 7. The A-side detector was extracted from the box, the vacuum sealing interface cleaned and the o-ring replaced before re-inserting the detector. At the same time the shims were removed, placing finally the VELO sensors at the nominal 5.1 mm from the beam. In this position, the uncertainty on the impact parameter, a variable that quantifies how displaced are particles from the primary interaction, and is thus critical for the LHCb physics programme, is expected to improve by 10%.

In the October 2024 report it was mentioned that the VELO motion system belt had to be changed in July 2024 after a damage, likely related to the 2023 vacuum incident, developed into a critical non-conformity. The belts available for the intervention were slightly smaller than the nominal ones, requiring to adapt the tension. The YETS 2024/25 was the occasion to replace the motion belts with properly sized ones and restore the system to its original design.

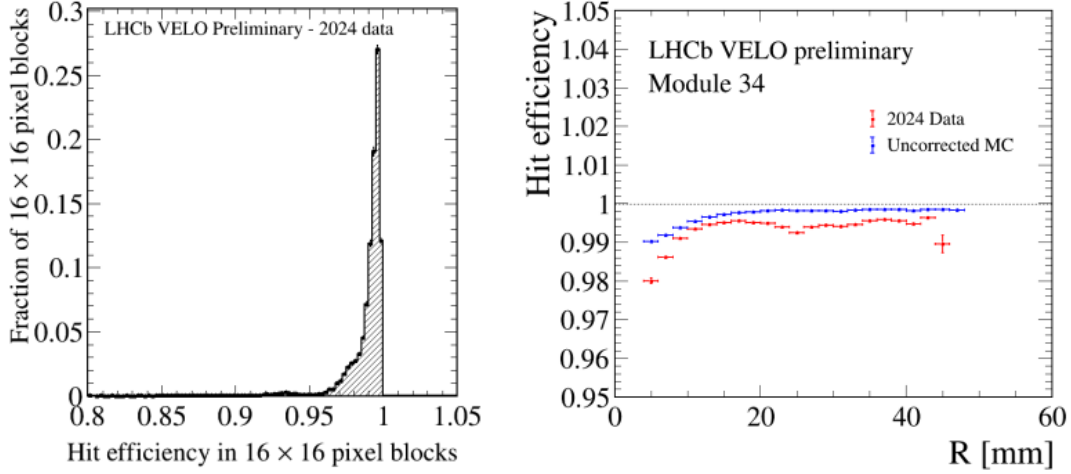


Figure 8: Left: The 41 million pixels are grouped into 16x16 pixel blocks and the hit efficiency is measured in data in each of those blocks. The efficiencies are shown in an histogram, and are weighted by the frequency the block is hit. Left: Hit efficiency as function of the radial distance to the beam in the module 34 of the VELO, in red as measured in data and in blue as implemented in the simulation. The simulation will be corrected by the value measured in data.

8.1.2 Operation and performance studies

In 2024 the VELO was operated with more than 98% of active links. While a biased hit efficiency, estimated from the presence of hit-on-tracks, has been used to monitor the performances during data taking, the full unbiased hit efficiency has been studied offline. Single hit efficiencies are well above 98% for most regions of the detector 8. With the delivered luminosity in 2024 the effects of radiation damage of the sensors start affecting the detector behaviour. In particular, while the total number of charge deposited by a track in the VELO sensors is large with respect to the pixel threshold, when they are shared over several pixels, some may be below threshold. As a consequence the average cluster size decreases with the increased received fluence, as illustrated in Fig. 9. The loss in depletion depth can be compensated by operating the sensors at an increased high-voltage. As illustrated in Fig. 9, as the bias voltage is increased, the depletion volume recovers and the fraction of single pixel cluster decreases while the pixels with close-to-threshold charges are recovered. High voltage scans allow to determine the optimal operation voltage at a given fluence while the evolution of the cluster size is used as a figure of merit to know when to update the voltages. In 2024 a single update of the high voltage was necessary, since only a small dependence of the hit efficiency was found as function of the radial distance of the hits, as seen in the Fig. 8, but in 2025 the process will be automated to minimise the effect even further.

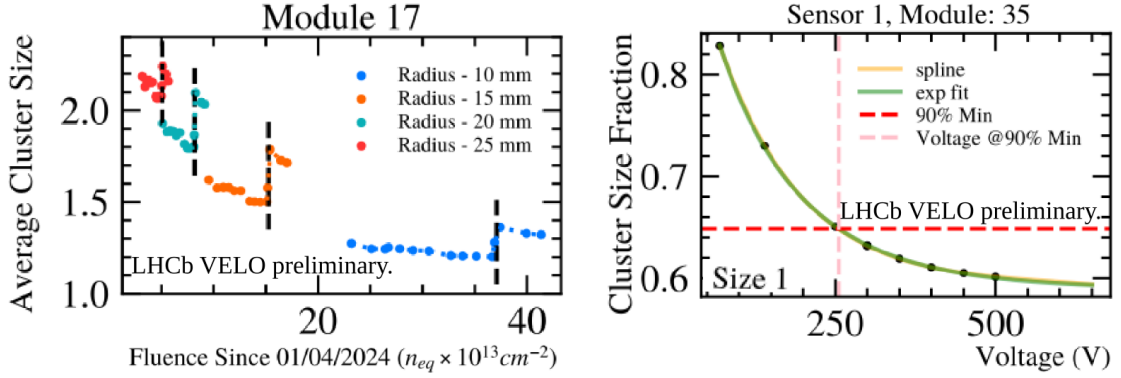


Figure 9: Left: the average cluster size is shown as function of the fluence received at a given position or the pixels. The black vertical line shows the moment where the high-voltage settings were increased to mitigate radiation damage. Right: At the end of 2024, the fraction of clusters with a single pixel decreases with the increase of the sensor high-voltage bias compensating for the effect of the radiation.

8.1.3 SMOG2

Running SMOG2, the only fixed-target gas system at the LHC, simultaneously with the beam-beam collisions has become the baseline operation mode for LHCb. The system has consistently demonstrated optimal performance for both the beam-gas and beam-beam events, provided that the two colliding systems can operate simultaneously without interference.

A major hardware upgrade was carried out during the winter shutdown, replacing the low-pressure gas reservoir (1.5 bar) with high-pressure gas bottles (200 bar). This upgrade brings key advantages. For instance, the preparation of the gas-feed system before the injection will now be quicker and more stable. Additionally, the system will no longer run out of gas during data taking, avoiding the need for repeated refills as experienced in the past. The PLC SCADA software has also been upgraded. Before, only one calibrated injection point per gas type was available, allowing only a predetermined and calibrated gas flow. Starting from the 2025 data taking, each of the four installed gases (hydrogen/deuterium, helium, neon, argon) will support low, medium, and high injection flux options. Moreover, a fine tuning feature allows adjustments in 2% steps, up to $\pm 20\%$ of the selected flux. This provides significantly greater flexibility in tuning the SMOG activity as a function of the beam conditions.

An online instantaneous luminosity monitor has been implemented in the control panels. For higher precision, targeting an accuracy of around 2%, ongoing studies aim to better parametrise the behaviour of the injected gas flow decay. Trigger lines and reconstruction algorithms have been further optimised, enabling high-efficiency event reconstruction for the upcoming data taking. Gas injections are foreseen already from the initial phases of LHC and LHCb commissioning, for producing activity even with low beam currents and during the van der Meer

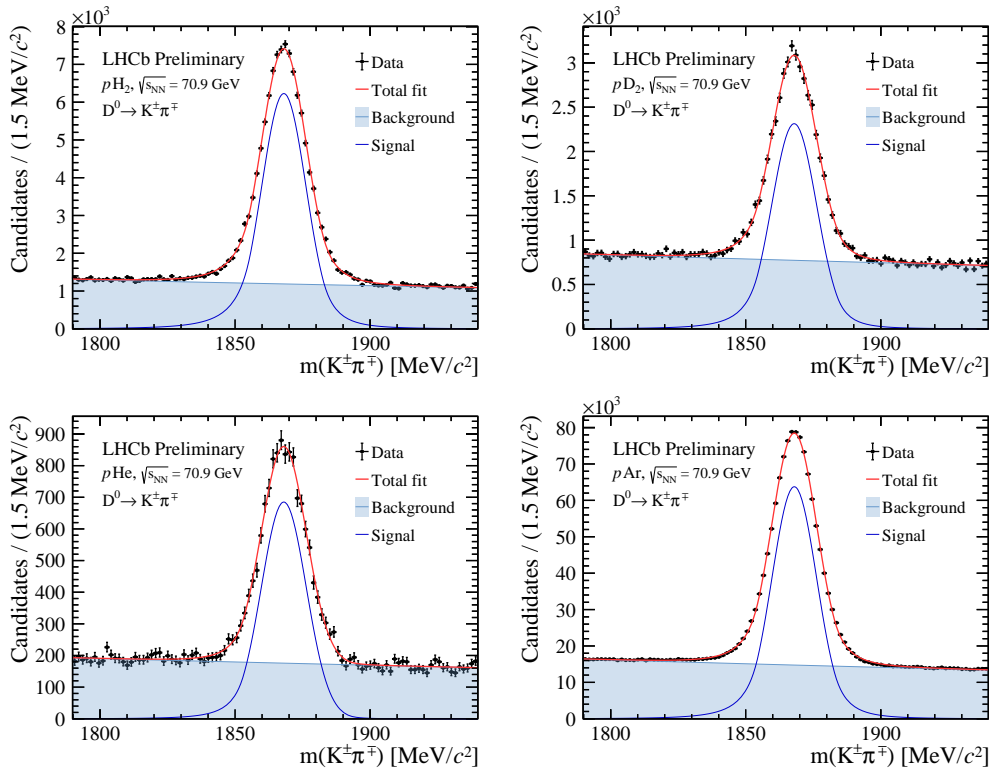


Figure 10: $K^-\pi^+$ invariant mass spectra using data from (left to right) $p\text{H}_2$, $p\text{D}_2$, $p\text{He}$, and $p\text{Ar}$ collisions collected during the pp reference runs at $\sqrt{s_{NN}}=70.9$ GeV. The gas injection durations are 16 hours for $p\text{H}_2$, 2 hours for $p\text{D}_2$, 4 hours for $p\text{He}$ and 56 hours for $p\text{Ar}$.

scans. Injections will also support beam-gas imaging (BGI) for LHC luminosity determination and ghost charges evaluations, not only for LHCb, but also for the other LHC experiments. The large statistics collected in 2024 using the various gas target are summarised in Fig. 3, while in Fig. 10 the $K - \pi +$ invariant mass spectra are reported, using data from $p\text{H}_2$, $p\text{D}_2$, $p\text{He}$, and $p\text{Ar}$ collisions collected during the pp reference runs at $\sqrt{s_{NN}}=70.9$ GeV. A detailed technical publication on the SMOG2 system and its initial performance is available in Ref. [47], and was selected both as an Editors' Suggestion and a highlight by the American Physical Society.

8.2 Upstream Tracker (UT)

8.2.1 Introduction and overview

The UT is a silicon microstrip tracking detector located between RICH1 and the dipole magnet of LHCb. It comprises four planes of vertical columns called staves. Each staff is a carbon-fibre structure with embedded Ti pipes to provide evaporative CO_2 cooling that hosts silicon front-end (FE) hybrid modules attached

to both sides to achieve full acceptance in the vertical direction. The dedicated (SALT) front-end ASICs, assembled on the 4 ASIC hybrids, feature 128 processing channels, including a low-noise preamplifier and shaper, and a 6 bit analog-to-digital converter (ADC). The digitised information is processed in a complex DSP, performing common-mode suppression and zero suppression for the normal data-taking operation.

8.2.2 2024 Heavy Ion Run

The UT detector was installed in the LHCb before 2023 run. However, because of the initial problems with the stability of its DAQ system, it was included in physics data taking only in 2024. Its performance at the designed pp luminosity was still limited by TELL40 DAQ boards, which were not able to handle the full hit rate in some parts of the detector, in the transition region from higher to lower granularity of readout elements in particular. Stable running was achieved by limiting hit rates from the ASICs by raising ADC thresholds and tightening hit limits in location dependent scheme. TELL40 firmware was equipped with self-protection mechanism preventing internal memory overruns by disabling new hit traffic until buffers emptied. Both mechanisms led to a moderate loss of UT efficiency of about 3.1% per long track.

The Heavy Ion PbPb run in fall 2024 produced events with track multiplicities varying from low to an order of magnitude higher than the pp collisions. However, luminosity during Heavy Ion runs was orders of magnitude lower, which made it possible to set the low ADC thresholds and very loose hit limits in SALT ASICs, with plenty of time in between busy events for TELL40 buffers to recover without loss of efficiency. The UT efficiency reached 99% per long track in the PbPb run, limited only by a number of ASICs which had to be switched off for hardware related reasons (3.5% scattered among 4 layers).

8.2.3 YETS work

The UT could be open for hardware repairs only towards the end of YETS. During that time some broken control boards were replaced and a number of broken communication links investigated. Some ASICs were revived thanks to this intervention. Nevertheless, the fraction of disconnected ASICs has not been improved substantially as some connections are not easily accessible. Risk-benefit assessment will be performed when planning for accessing these areas during LS3.

During 2024 run, cooling of UT detector was limited to -10°C due to too much moisture penetrating the UT enclosure in summer months. This was due to the large leaks from the UT box through the peripheral electronic volume on top and bottom of the detector, as well as where the two halves of the UT box meet in closed position, and around the beam pipe flange. The sealing of the box was improved in all these areas. In addition, N2 flushing rate has been increased by about 25%. The detector can now be safely operated down to -20°C through entire

year. Via extensive electronic calibrations and tests performed during the YETS, we decided to operate UT at -15°C in 2025. This offers most of the improvement from lower electronic noise at colder temperatures, while avoiding pushing too many ASICs to operate close to their dynamic range limit.

A significant effort over the YETS went into resurrecting the “slice test” set-up used previously at CERN for testing of prototype staves and readout boards. ECS and firmware were updated to the latest releases. Then the set-up was used to test and evaluate spare readout boards. It also offers a possibility to test new control software and TELL40 firmware prototypes without interfering with the main detector operations.

Electronic calibrations and scans have been sped-up by taking advantage of the new control options. Baseline noise studies, TrimDAC scans to optimize ASIC dynamic range settings, as well as pulse-shape calibrations using injected charge were performed at various cooling temperatures. They improved our understanding of the Front-End performance in various parts of the detector. Since the detector is now closed and the cooling is set to the new nominal temperature, electronic calibrations are now being performed in preparation for the beam-operations.

8.2.4 Progress in TELL40 firmware

New expert personpower was added to the UT TELL40 firmware development team over the YETS to overcome the efficiency limitations experienced during the 2024 pp run at the design luminosity. Significant improvement in the number of FPGA cycles needed to read out the frontend ASICs was implemented in the bunch-crossing alignment block, followed by similar changes in the data processing block formatting output raw data. Independently, the input buffers were doubled in length in the alignment part, which should move self-protection thresholds to higher hit rates. The tests on the firmware simulations are extremely encouraging. Testing with the real detector has started. Since simulations of prolonged data taking with all complexity of real detector conditions are not possible, only tests with real pp collisions at the design luminosity will show if the firmware improvements have been sufficient to operate UT at its full efficiency as in the 2024 PbPb run. If not, a new frontend tune of ADC thresholds and hit limits will need to be found. The outlook is very promising and we expect the 2025 pp data taking to improve over already good 2024 UT performances. The frontend setup is expected to be less fine-tuned, thus decoupling DAQ efficiency from the exact instantaneous luminosity value, making the detector more resilient to the conditions of SMOG injections.

8.3 Scintillating-Fibre Tracker (SciFi)

8.3.1 System overview

The technology and design of the SciFi system are described in the LHCb Tracker Upgrade TDR [5]. The active element of the SciFi consists of $250\ \mu\text{m}$ thick and

2.5 m long scintillating fibres arranged as hexagonally close-packed six-layer mats of 131 mm width. Eight of these mats are joined to form 5 m long and 52 cm wide modules. The fibres are read out from the outer ends by 128-channel arrays of silicon photomultipliers (SiPM), which can be cooled to -40°C to limit the single-pixel dark-count rate after irradiation. It is composed of a total of 524,288 read-out channels.

The fibre modules together with the readout electronics are mounted on $6\text{ m} \times 4\text{ m}$ large support frames (C-frames). These frames provide the necessary services (low voltage and bias voltage, optical connections, SiPMs cooling) including water cooling of the electronics. The necessary cooling of the SiPMs is achieved with a separated cooling system operated at temperatures as low as -50°C .

The detector is divided in half with 6 C-frames arranged in 3 stations of X-U V-X layers installed on each side of the beam-pipe; there are 12 C-frames in total. A survey system (BCAM) is used to monitor the movements of the C-frames over time in addition to the alignment with tracking data.

We have had a stable operation of the SciFi Tracker since 2023.

8.3.2 Detector operation and performances

SciFi has been running smoothly within the LHCb data acquisition system during 2024 and data-taking was very efficient. Only 4 out of 512 front-end electronics boards and a few links became faulty during the operation in 2024. Operation during the year was supported by 26 piquets, with the help of senior experts and more experienced piquets. Scrupulous refinement work to understand the detector has been undertaken to improve every channel where possible, and this work continues.

In 2023, we reached an average hit detection efficiency of all SiPMs close to 98 % and, as expected, a better understanding of SciFi allowed us to achieve the highest performances in 2024 as this is seen in Fig. 11 for two fills near the end of the running period. The majority of the pp physics will have a similar efficiency to Fill 10213. The average hit efficiency in the layer under study in Fill 10213, averaged over all layers, for tracks traversing the modules nearest the beam pipe is $99.0^{+0.3}_{-0.4}\%$ (edge channels excluded, accidental matches included). A second-order polynomial is fit in order to project the performance to a lower number of hits in the layer, in order to remove effects from accidental matching and ghost tracks, producing a value similar to seen in test-beam measurements.

An update to the thresholds during the machine development before the heavy-ion run resulted in slightly improved efficiencies for the M0 modules, as see from the data for Fill 10310. The average hit efficiency in the layer under study in Fill 10310, during the pp reference run, averaged over all layers, for tracks traversing the modules nearest the beam pipe is $99.2^{+0.2}_{-0.3}\%$ (edge channels excluded, accidental matches included).

The number of additional clusters in the following bunch crossing has also been reduced in July 2024 by 1/3, by fine tuning the thresholds without a noticeable

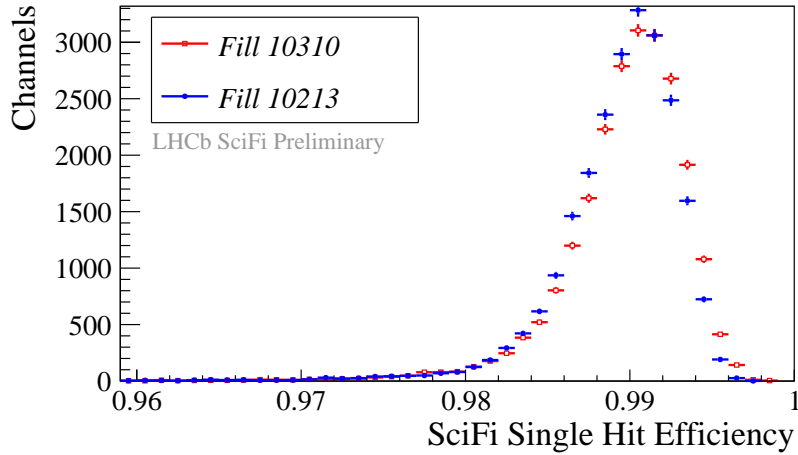
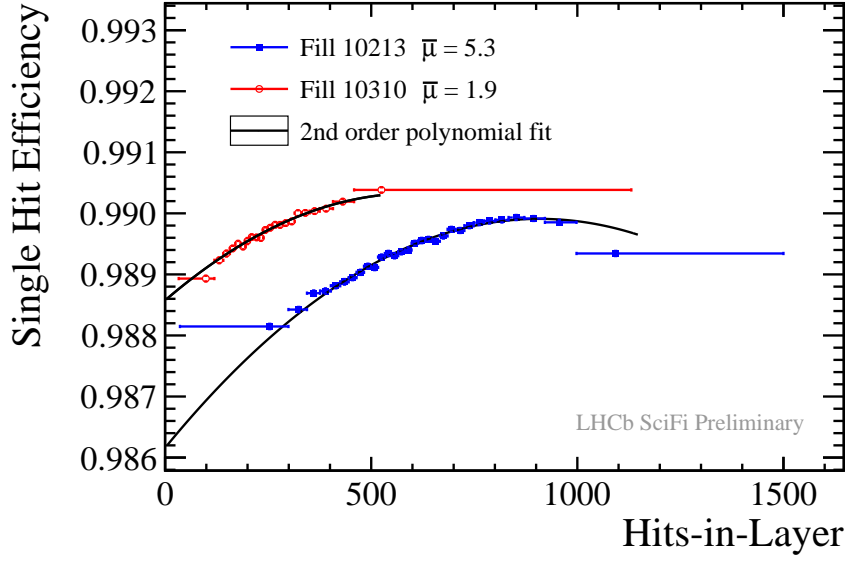


Figure 11: Unbiased hit efficiency as a function of the number of hits in the layer under study, averaged over all layers, for the LHCb Scintillating Fibre Tracker. Data are presented for two LHC fills from late 2024 (Fill 10213 and Fill 10310). Only long tracks traversing the M0 modules (nearest the beam pipe) and with track positions at least two channels away from the sensor edges are considered. Tracks are required to satisfy $p > 10$ GeV, $p_T > 400$ MeV, GhostProbability < 0.02 , nUTHits = 4, and nFTHits = 11. The efficiency is defined as the probability of finding a cluster hit within 1.5 mm of the interpolated track position at the layer under study. The increasing trend is attributed to a higher likelihood of accidental matches with rising occupancy, while the higher efficiency in Fill 10310 is associated with improved threshold tuning during the machine development preceding the proton-proton reference run before ion beams.

impact on efficiency.

We are also investigating methods of determining the light yield loss due to irradiation in-situ using non-zero suppressed data during beam collisions, and have also planned a measurement for the next YETS to measure the light yield with a radioactive source using a custom readout electronics provided that has been used in test-beams.

Additional information on the performances of the SciFi detector in the tracking system is given in section 12. A SciFi Detector performance paper is being written and will be submitted this summer for publication.

8.3.3 Maintenance activities during YETS

Several activities took place during the Year End Technical Stop 2024/25. A first week of continued operation of the detector was used to debug operational matters in software, and in parallel a temperature controlled annealing of the SiPMs were also performed to verify the annealing speed. Silicon photo-multipliers (SiPMs) are radiation-sensitive. Radiation causes defects in the silicon lattice, creating intermediate energy states leading to an increased probability of thermal excitation and thus of free charge carriers generation. These carriers trigger avalanches in individual pixels. In the absence of light, this single pixel background signal is known as the dark count rate (DCR). Crosstalk between pixels, with a probability of a few percent, as well as separate pixels overlapping-in-time, can create signals greater than 1 p.e. that look similar to real hits with low amplitude and can pass the thresholds to produce clusters.

The reconstructed dark clusters induced by the DCR are monitored during the year with dedicated noise runs, and currently produce less than 100 extra clusters per bunch crossing and are negligible in regards to the tracking performance at the moment. They will become more significant in Run 4.

Figure 12 (left) shows the evolution of the DCR for the 3 SciFi station as a function of the delivered luminosity. The linear increase of the DCR with the delivered luminosity is interrupted by partial annealing periods, highlighted in gray dashed lines, where the detector was operated warm at $\sim 25^\circ\text{C}$, leading to a decrease of the DCR. At the end of 2024 operations, a DCR of 4.2 MHz at 12.5fb^{-1} has been measured for the more irradiated region (T3L3M0). During the YETS, the detector has been warmed at room temperature ($\sim 20^\circ\text{C}$) for a period of 55 days after which the detector is expected to be fully annealed. In Fig. 12 (right), the DCR measured at these three specific points, before, during and after annealing, is shown. A reduction of around 40% is observed over a period of 55 days. In the most irradiated region of the detector (T3L3M0), a DCR of 2 MHz is measured after annealing, which is in line with the expectation from R&D.

Improvement and preparation of the operation in 2025 were pursued, full detector electronic internal clock scans were carried out as well as further investigations and improvement of the Light Injection System for threshold calibration.

The last part of the Condensation Prevention System (CPS) upgrade was per-

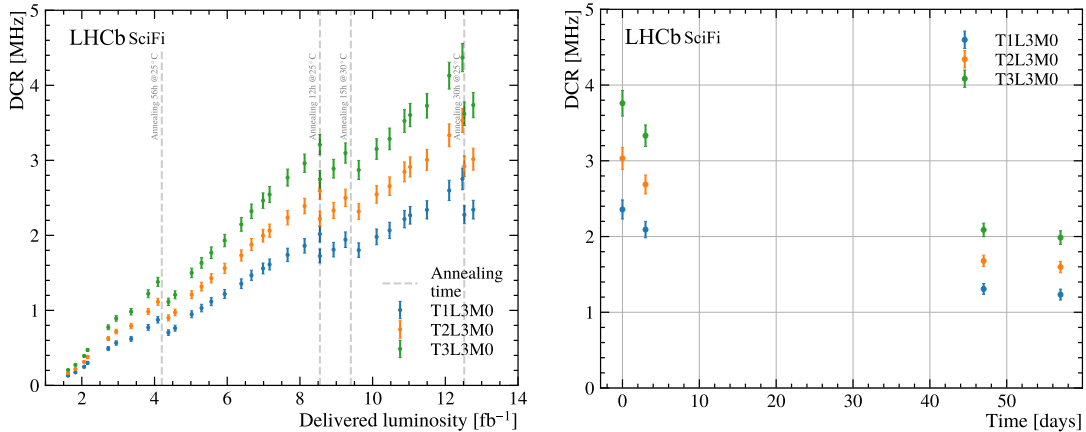


Figure 12: Left: Dark Count Rate (DCR) per SiPM channel as a function of the delivered luminosity. The points shows an average DCR over the SiPMs. Right: DCR before, during and after full annealing of the detector at room temperature ($\sim 20^\circ\text{C}$). Measurements are shown for the innermost module (M0) of the thirds layer (L3) for the first (in blue), second (in orange) and last (in green) station of the SciFi detector.

formed to make it more robust against faults, as the detector must be warmed up if the CPS fails. The upgrade consisted of removing all 48 monitoring boards from the C-frames and replacing them with a new version with various improvements. The main improvement was the multiplexing of the current source for the temperature sensors, which makes all the sensors fully independent. Another part of the CPS upgrade was the introduction of a fuse board on the back plane of the C-frames. This allows the fuses for the heating wires to be replaced without opening the C-frames and allows to fully disconnect a heating wire, which speeds up debugging substantially. Overall, 48 cables were also changed on the C-frames to modify the granularity of the heating wire power to match the granularity of disconnection of cooling. This will minimize the part of the detector to be operated warm in the unlikely event of a problem.

Following a positive evaluation of a different cooling liquid for the SiPM, called NOVEC 7100, with a lower greenhouse warming potential ($\text{GWP}=300$), the former cooling liquid C_6F_{14} ($\text{GWP} = 10,000$) was removed and replaced by NOVEC 7100, which means a reduction of GWP of 97 %.

The various services had the usual annual maintenance like replacing vacuum pumps, clean water filter, maintain cooling plants (PSU cooling, FEB cooling and SiPM cooling). A few temperature sensors (2 of 624) and flow meters (2 of 512) were also recovered, such that all sensors are currently operational. 2 Front-End boards (FEB) were also replaced.

Lastly, a major campaign to clean all control fibres connected to VTRx transmitters was made in the YETS. This is due to a known issue where the remainder of the unhardened epoxy component used in the construction of the VTRx out-gasses

when heated during operation. The vapour condenses on the optical control fibre end, which eventually degrades the transmission to the point of failure. This issue can be fixed by baking the VTRx transmitters, but most of the SciFi electronics were already installed, and difficult to remove, where the installations schedule did not allow for replacement of the majority of the transmitters.

Before cleaning the control fibres, all were checked with a fibre microscope to keep track of the debris from the out-gassing. The access to some of many of the fibres is very difficult and has a significant overhead of mechanical preparations and, *e.g.*, implying multiple positions of the C-frames to access a single fibre. Around 700 fibres (including all connected to unbaked VTRx) were cleaned during the YETS. Around 100 fibres had liquid from the outgassing varying from a little deposit to a huge amount for ~ 30 fibres. 4 FEB became non operational during part of the 2024 operation due to this effect. Currently, after the cleaning campaign, all control fibres are operational. There are only 2 excluded data links left ($\sim 0.05\%$ of SciFi) for data taking in 2025.

This cleaning will likely need to be repeated every YETS to ensure good operational efficiency.

9 Particle identification detectors

9.1 Cherenkov detectors (RICH)

9.1.1 System overview

The RICH system of LHCb is composed of two detectors, RICH1 and RICH2, designed to provide charged hadron identification in the momentum range 2.6 – 100 GeV. The upgrade of the RICH system consists of new optics and mechanics for the RICH1 detector and new opto-electronics chain in both RICH1 and RICH2. The new opto-electronics chain is composed of multi-anode photomultipliers (MaPMTs) as photon detectors, read out by a custom ASIC, the CLARO chip, designed to digitise the signal at 40 MHz. Finally, a FPGA-based digital electronics takes care of the interface with the PCIe40 for both the trigger and fast control and the data transmission. The full installation of the upgraded RICH system was achieved during LS2, with RICH2 being the first sensitive element installed for the entire LHCb Upgrade, so that both detectors were ready to be operated at the start of Run 3.

9.1.2 Maintenance and YETS activities

During the YETS period, the RICH team performed regular maintenance on the RICH detectors. The year 2024 was the first year of nominal data taking. As a consequence, the team organised an intervention for qualitative inspection of all the Photon Detector Modules (PDM). A dedicated campaign was organised to inspect each column of the RICH1 detector, with particular focus on the MaPMT

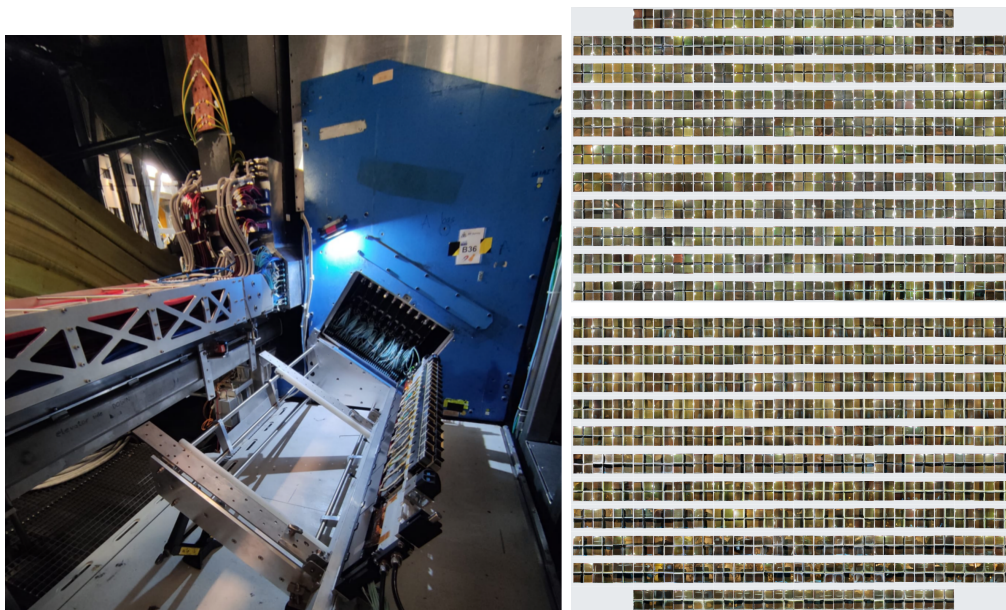


Figure 13: Left: extraction of the RICH1 columns in the Down enclosure for inspection. Right: overview of all the MaPMTs inspected during the YETS from both the Up and Down enclosures.

windows, for both the Down (November) and Up (January) enclosures. The procedure and result are shown in Fig. 13: on the left an extracted column from the Down enclosure while on the right the composed picture of all MaPMTs installed in RICH1 are shown. This intervention confirmed the healthy status of the detector and was possible thanks to the constant support that the team receives from the collaborators dedicated to Maintenance & Operations activities. This, only apparently, huge intervention was conducted in a total of six working days, demonstrating once again the successful redesign of the photon detector enclosures of the RICH Upgrade which greatly facilitates interventions.

Minor interventions were also performed on the optoelectronics chain in RICH1, with a focus on few digital readout boards.

A dedicated campaign of inspection of the optical links was carried out on the RICH2 detector in February. During LS2, the out-gassing phenomenon affecting the VTRx was discovered. While the RICH1 detector was equipped with "baked", not affected, VTRx components, the RICH2 detector had already been installed, hence it is fully equipped with links who could be negatively affected by out-gassing. While the optical transmission is constantly monitored and no big effects have been observed on the data taking stability, the RICH team decided to carry out an inspection on a random sample of VTRx in RICH2. The outcome is coherent with the observations by other sub-systems, such as the SciFi detector. Cleaning of the optical fibres was performed accordingly.

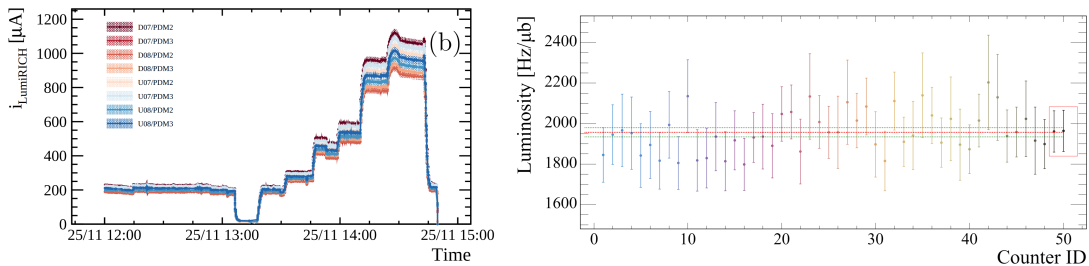


Figure 14: Left: the trends of the RICH luminosity counter provided by the anodic current, for the eight PDMs in the high-occupancy region of RICH1 during a luminosity scan. Right: Luminosity estimated from a subset of 48 hit counters, equally divided between RICH1 (leftmost) and RICH2 (rightmost); the last two values, highlighted in the red box, are obtained using the number of VELO tracks as luminosity counters.

9.1.3 Performance and readiness for data taking

The RICH system has been operating stably since the beginning of Run 3. Already at the end of 2022, the RICH system could provide an improved performance compared to Run 2 [48]. The unprecedented Particle Identification (PID) capability was confirmed throughout 2024, running in nominal conditions of instantaneous luminosity [49]. The excellent performance of the RICH system has allowed the community to perform dedicated calibration studies in view of the phase II Upgrade of the LHCb experiment, such as operations with different timing windows or High Voltage settings.

At the end of 2024, after a record year in terms of integrated luminosity, particular care has been devoted to the study of possible ageing of the MaPMTs. The main parameter under study is the photon detector gain. For this reason, regular campaigns of threshold scans are performed and, so far, no major or unexpected ageing has been observed. The next campaign will take place during the LHC intensity ramp up in spring 2025, to evaluate the possibility of tuning the operating parameters for the data taking.

The Upgrade of the RICH opto-electronics chain, in particular the usage of the MaPMTs, has opened the possibility for the RICH system to provide counters proportional to the instantaneous luminosity. The team, in collaboration with the LHCb Luminosity Working Group, has performed calibration studies of such counters since the beginning of Run 3 (see Fig. 14). This studies have converged in the first detector publication submitted to journal on Run 3 data, across the LHCb community [50], showcasing the excellent quality of the RICH system, beyond the PID measurements.

9.2 Calorimeters (ECAL and HCAL)

9.2.1 System overview

The upgrade of the LHCb calorimeters consisted in replacing the electromagnetic (ECAL) and hadronic (HCAL) calorimeter readout electronics and upgrading the high-voltage, monitoring and calibration systems. The detector modules of the original LHCb were retained. The gain of the photomultipliers (PMT) has been reduced by a factor up to five in order to keep them operational throughout the higher luminosity runs of the upgrade. The new analogue electronics partially compensates for the gain reduction by boosting the signals by a factor of 2.5. The remaining factor of two is used to extend the dynamic range of the calorimeter system and thus to extend the physics case to some new topics.

The construction of the electronics, for the front-end, the high-voltage, the monitoring and the calibration of the calorimeters was completed in 2021. After the productions, the installation started in parallel with the tests of the hardware, so that the installation was achieved the same year. The final firmware versions to ensure a proper processing of the electronics have been written and loaded also in 2021.

The commissioning started then. The consolidation of the system was done in parallel with the fine-tuning of the configuration, adjustments and the first steps of the calibrations. The ECAL and HCAL detectors are fully operational and are used routinely in the global LHCb acquisition since Spring 2022. The calorimeters took part in the first high-energy collisions in stable beams in July of the same year. We are routinely and smoothly running the ECAL and HCAL with a very high efficiency.

9.2.2 Maintenance over YETS

We used the period of the Winter technical stop to perform some important maintenance operations on the detector.

The ECAL Cockcroft-Walton (CW) bases cannot accumulate more than 10 Gy without having their performances affected. Hence, we estimated the dose reached by each base of the ECAL in 2025. Those that are expected to overtake 10 Gy have been desoldered from their PMT, removed and replaced by spares. This is an operation that is foreseen, and we have sufficient spares for the life of the detector. In total 204 PMT (102 per side) have been replaced.

The HCAL bases do not experience such a dose problem. But, we have to watch for the dark current of the photo-multipliers which is constantly monitored. A total of 21 PMT had to be removed during the Winter shutdown, 14 on the C side and 7 on the A side of the detector, because of a dark current exceeding the specifications. In order to speed up the operation, spare PMT had been already prepared with bases which had been removed from the HCAL last year. The new systems PMT-base have been installed on the HCAL. The removed bases will be soon desoldered from their PMT in order to be used with spare PMT next year.

Once again, this is an operation which is planned, and we have enough spare for the life of the calorimeter system.

At the end of the 2024 run, two e-links connectors of two boards used to produce the LED pulses of the ECAL calibration system were unstable. They have been fixed and tested. Moreover, a LED driver, on C Side of the HCAL had to be replaced.

A few channels are dead or noisy at the level of a few per mille. We benefit from technical stops to regularly cure the corresponding problems. The main origin for the fault comes from a bad connection on the input connector of the front-end electronics. However, several ECAL/HCAL front-end boards had to be replaced. And a control unit (3CU board) was unstable and has been replaced also.

9.2.3 Calibration

The ECAL and HCAL energy calibrations are performed routinely and satisfactorily. The HCAL uses a cesium source which got stuck into its garage during the last 2023-2024 Winter campaign of calibration. After the cleaning of the radioactive capsule by the radioprotection service at CERN, we did several calibration runs in 2024 without any issue. A recent Cs source calibration took place end of March 2025, before the closure of the cavern, and was also successful.

The time alignment of the ECAL and HCAL channels is now a routine operation. In order to start the 2025 data taking period in good conditions, we did a TAE run at the end of the 2024 period, which was also successful and permitted to check the individual time configuration of the channels.

The ECAL energy calibration is usually done by reconstructing neutral pions. However, this requires a large sample of data and could not be done at every fill, inducing a noticeable decrease of the response of the ECAL in between calibrations. We have now added a relative calibration, applied at each fill, based on the response of the calorimeter channels to the LED pulses. The combination of the two calibrations, absolute and relative, permits to stabilize the response of the detector in spite of the high multiplicity reached during the crossings at high μ , that we experience since a couple of months.

9.2.4 Reconstruction and monitoring

At the end of 2024, a non-linear response of the ECAL has been observed with respect to the energy, and in the innermost region of the detector, close to the beam pipe. This is the region for which the occupancy is the largest one, and we also expect to start to observe some ageing effects in the calorimeter modules, due to the accumulated dose. Work is ongoing to modify the reconstruction, in order to improve the mitigation with respect to the occupancy and to solve the non-linear effect. Some corrections are foreseen and should be implemented in the software to compensate for the non-linearities seen.

There has been some work recently to improve the alarms triggered by the

monitoring system of the calorimeters. The monitoring has also been improved by adding new histograms that should ease the work of the experts and LHCb shift crews.

9.3 Muon chambers (MUON)

The MUON detector has performed exceptionally well in Run-1 and Run-2. The main changes for Run-3 are the removal of the M1 layer, the redesign of the off-detector electronics, and the installation of a new shielding in front of the inner region of M2 to reduce by about a factor two the low energy background rate in this region.

The electronics of the MUON detector upgrade consists of a new readout board (nODE), equipped with four custom ASICs (nSYNC) redesigned to be compliant with the 40 MHz readout of the detector, and of new control boards, the Service Board (nSB) and the Pulse Distribution Module (nPDM), redesigned to be compliant with the new ECS/TFC system.

The MUON system is successfully taking part in the Run-3 LHCb data taking. The detector has been working well. The experimental control system (ECS) has been in daily use to operate and control the MUON system. A lot of effort has been put on the optimisation of the DAQ and in its interaction with the TELL40 firmware. A suite of new ECS panels has been developed to help this optimisation and serve as tools for the piquets and the experts in the management of the system. The new version of the online monitoring has been enriched with new histograms and with the activation of automatic analysis. The MUON TELL40 desynchronisation caused large inefficiencies in 2022. The root cause of the desynchronisation is still being investigated, but many tests allowed a working configuration for power supply, firmware, and software to be found, such that the issue is reduced to a negligible level, no longer affecting either the DAQ or muon identification performances. The MUON system has been aligned to the LHC clock, and the procedure for the fine time alignment of the electronics within the 25 ns bunch has been completed using the high quality Time Alignment Events data have been collected at the beginning of the 2024 data taking, allowing near-nominal performance.

During the last YETS the few issues appeared during 2024 data taking have been fixed, including the replacement of four MWPC.

A lot of effort has been also put to update the Run-1 and Run-2 MUON software to the Run-3 detector and environment. The readout cabling was changed and that required a new raw data decoding and simulation encoding software. The reconstruction and identification algorithms have been adapted to the tight time constraints of the full software trigger. The improvement of the tracking system and of the muon time-alignment allowed good identification performance to be reached.

The removal of M1 and the new shielding required to modify the detector description, and all the geometry has been ported to DD4HEP, and the work to port to DD4HEP all methods has been recently completed. Finally an improved

modelling of the detector response to low energy background and to spillover is ready to be used in the simulation.

10 PLUME and luminosity

The LHCb Upgrade-I detector has been equipped with dedicated systems whose goals are to continuously monitor luminosity and beam-induced background conditions. Moreover, other LHCb sub-detectors started to provide ECS counters to monitor the luminosity, increasing redundancy.

10.1 System overview

The luminosity and beam/background monitors at LHCb are composed of a set of hardware- and software-based systems. The PLUME detector is a new detector based on a set of photomultipliers (PMTs) with quartz radiators, using the calorimeter front-end readout electronics specifically adapted for Run-3. PLUME is fully dedicated to monitor in real-time the instantaneous luminosity, averaged and per bunch, and to provide a direct measure of the average number of visible pp interactions per bunch crossing (μ). PLUME is synchronised with the LHC clock and in addition it is included in the LHCb Data Acquisition (DAQ) system providing such measurements for offline purposes included in the event bank.

The VELO dedicated read-out, based on the Retina clustering algorithm that runs on the VELO FPGAs, provides reconstructed clusters at the earliest stage of the DAQ chain, enabling efficient monitoring of luminosity in real time by measuring sensor occupancy. A set of counting regions serve as luminosity counters, which are calibrated with van der Meer (vdM) scans.

The Beam Conditions Monitor (BCM) directly measures beam losses around the LHCb interaction region and acts as the LHCb primary safety interlock, dumping the beams when such losses are above specified thresholds. The BCM consists of two stations (Upstream and Downstream), each composed of 8 diamond sensors interfaced to current-to-frequency converter (CFC) cards providing continuous running sums (RS) over 40 μ s (short RS) and 1280 μ s (long RS).

The Radiation Monitoring System (RMS) continuously estimates the amount of beam-induced losses observed around the LHCb interaction region. The RMS is composed of 4 stations, each composed of 2 metal foil detectors connected to charge-to-frequency converters. The change in frequency is linearly proportional to the number of minimum ionising particles (MIPs) providing an estimate of the amount of particles lost by the beams around LHCb.

PLUME, BCM Upstream and RMS are located around 1.5 m from the interaction point, in the zone between the VELO and the cavern wall, commonly referred to as the VELO alcove. The BCM Downstream system is located between the Upstream Tracker and the LHCb dipole.

10.2 PLUME-based online luminosity

The main improvements achieved in 2024 are listed below.

- **Background subtraction:** to achieve a precise luminosity determination, the contribution from SMOG2 must be subtracted from that of pp or PbPb collisions. The background subtraction formula used is

$$\mu_{\text{bkg.sub.}} = \mu_{bb} - \mu_{be} - \mu_{eb} + \mu_{ee}, \quad (1)$$

where the various μ_x , with $x = bb, be, eb$, or ee , indicate the average number of detected collisions in beam-beam, beam-empty, empty-beam, and empty-empty crossings, respectively. The former includes contributions from pp or PbPb collisions as well those between the beams and the injected gas. Reliable proxies for subtracting these latter components are μ_{be} and μ_{eb} , where only beam-gas and gas-beam collisions are expected to occur, respectively. Moreover, since the beam populations in beam-empty and empty-beam crossings decay differently from those in beam-beam crossings, a correction factor is applied to μ_{be} and μ_{eb} . Lastly, the background arising from interactions with the residual gas in the LHC beam pipe are accounted for by the μ_{ee} term.

Figure 15 shows the background-subtracted μ , along with the individual components appearing in Eq. (1), for two fills of the 2024 pp and ion runs, respectively. As shown, due to the significantly lower instantaneous luminosity achieved during the ion run, a precise background subtraction becomes considerably more important. Imperfections in the background subtraction as large as 7% of the μ_{eb} contribution are observed in $\mu_{\text{bkg.sub.}}$ when gas is injected into the SMOG2 cell, depending on the type of gas used. The origin of this effect is still unclear and currently under investigation.

- **Photomultiplier gain stability and ageing:** ensuring detector stability throughout the entire data taking period is crucial. Any unaccounted variations in PMT gain could compromise the vdM calibration, making it essential to maintain stable operating conditions for the PMTs. To achieve this, a dedicated procedure has been developed. At the end of each physics fill, the ADC spectra from all PMTs, as recorded by the LHCb monitoring system, are gathered and a fitting model is adapted to the data. An example of such fits is shown in the top left of Fig. 16. To ensure gain stability, the fit determines the position of the peak in the ADC spectrum corresponding to particles impinging quasi-perpendicularly on the PMT windows. This peak is expected to be centred at 300 ADC counts when the gain is maintained at 1.5×10^5 . The top right panel of Fig. 16 displays the peak position as a function of the LHC fill number for PMT 2, as an example. The average deviation from the target value is of the order of 1%. The bottom panel presents the distribution of this peak for particles incident quasi-perpendicularly on

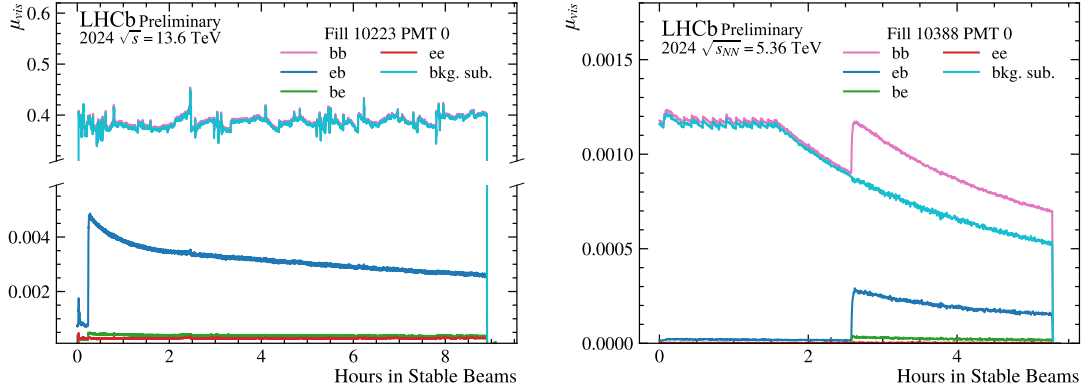


Figure 15: Average number of visible interactions measured by PMT 0, separated by bunch-crossing type and combined to obtain $\mu_{bkg.sub.}$ for (left) a pp and (right) PbPb fill.

the PMT quartz windows over the entire 2024 pp data taking period and for all PLUME PMTs. Any variation in the peak position, *i.e.* a variation in the PMT gain, translates directly into a bias in the instantaneous luminosity measurement. Since gain calibration is performed individually for each PMT, the uncertainty in the PLUME average instantaneous luminosity due to potential miscalibration is estimated using toy MC simulations to remain well below 1%.

The increase in the PMT high-voltage supply, resulting from the gain adjustment procedure, is continuously monitored to determine if any action is required during one of the LHC end-of-the year technical stops, such as replacing PMTs that reach the maximum allowed voltage (1375 V). Figure 17 shows the high voltage applied to keep constant the gain of PMTs as a function of the integrated charge collected by PMT 0 and PMT 8 during 2024. PMT 0, being one of the closest to the beam pipe, accumulated more charge, whereas PMT 8, positioned farther away, collected less. Assuming a similar charge accumulation during the 2025 and 2026 operational periods and extrapolating from the current trend, the high voltage supplied to the PMTs is expected to remain below the maximum tolerated level.

11 VELO-based online luminosity and beam-spot monitoring

In Run-3, the upgraded VELO detector at LHCb plays a key role in online luminosity measurement. Thanks to its new pixel technology and real-time readout at the 30 MHz LHC bunch-crossing rate, the VELO provides online hit information that is processed directly on the readout FPGAs. A set of 208 firmware counters (8 per station, 26 stations) tracks hit activity across the detector with high spatial

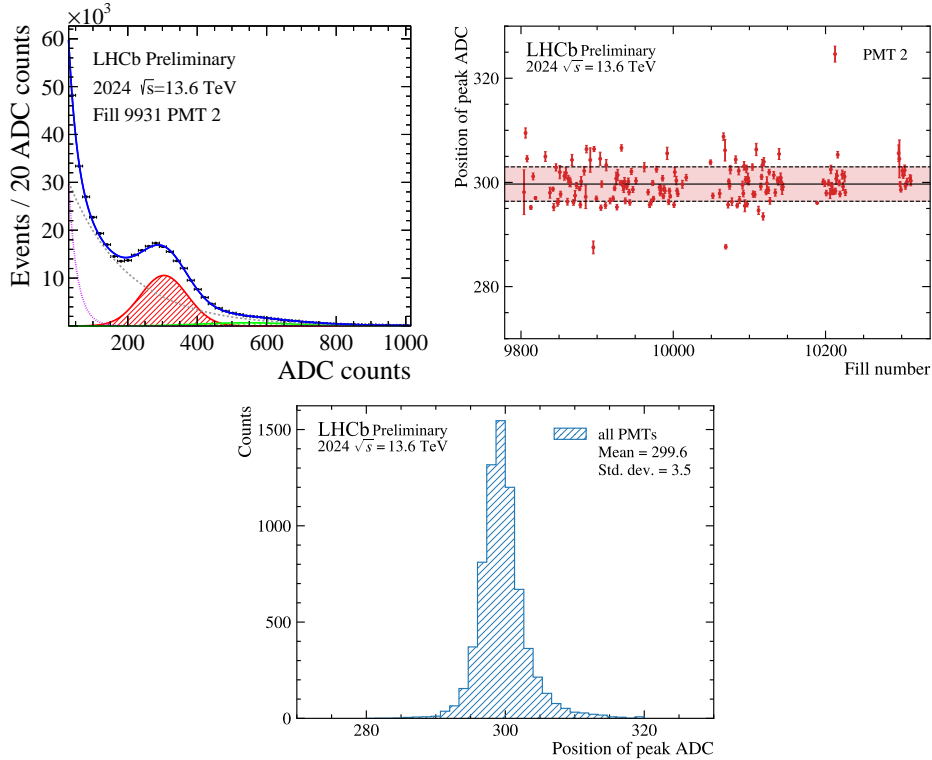


Figure 16: Top left: ADC spectrum obtained from the LHCb monitoring system for PMT 2 during LHC fill 9931, with the fit results overlaid. The Gaussian function (red dashed) describes the peak due to particles impinging quasi-perpendicularly on the PMT window. The other Gaussian function (green dashed) describes events in which 2 particles enter the PMT. The exponential components are used to model events in which one or more particles impinge on the PMT window with angles larger or smaller than 90 degrees. Top right: peak position for PMT 2 as a function of the LHC fill number. The central value and half-width of the red band are 299.7 and 3.3 ADC counts, respectively. Bottom: distribution of the peak due to particles entering the PMTs quartz window quasi-perpendicularly for the whole 2024 pp data taking period. Data from all PMTs is aggregated.

granularity.

These counters allow the use of both the *average* and *logZero* methods for luminosity extraction, offering robustness against effects such as radiation damage and changing detector conditions. Counters are read out every 3 s for integrated luminosity monitoring, and every 40 s for per-bunch analysis. Calibration is performed using dedicated vdM scans, and preliminary results show systematics at the level of 0.3–0.5%, with good agreement with the PLUME luminometer, as shown in Fig. 18).

Additionally, VELO-hit information is used to monitor the beam spot position in real time. By defining a linear estimator based on normalized hit distributions

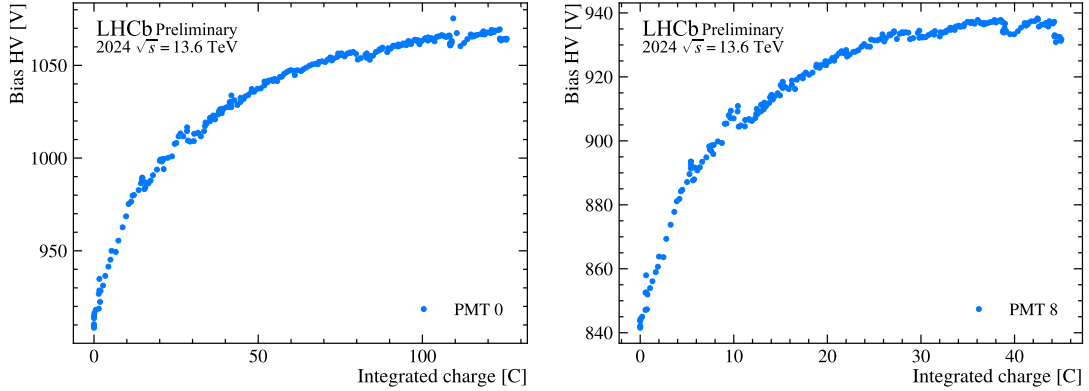


Figure 17: Bias HV applied to (left) PMT 0 and (right) PMT 8 to keep the gain constant versus the total charge collected by the same PMT. The correction to the HV is computed at the end of every LHC fill from the adjustment procedure.

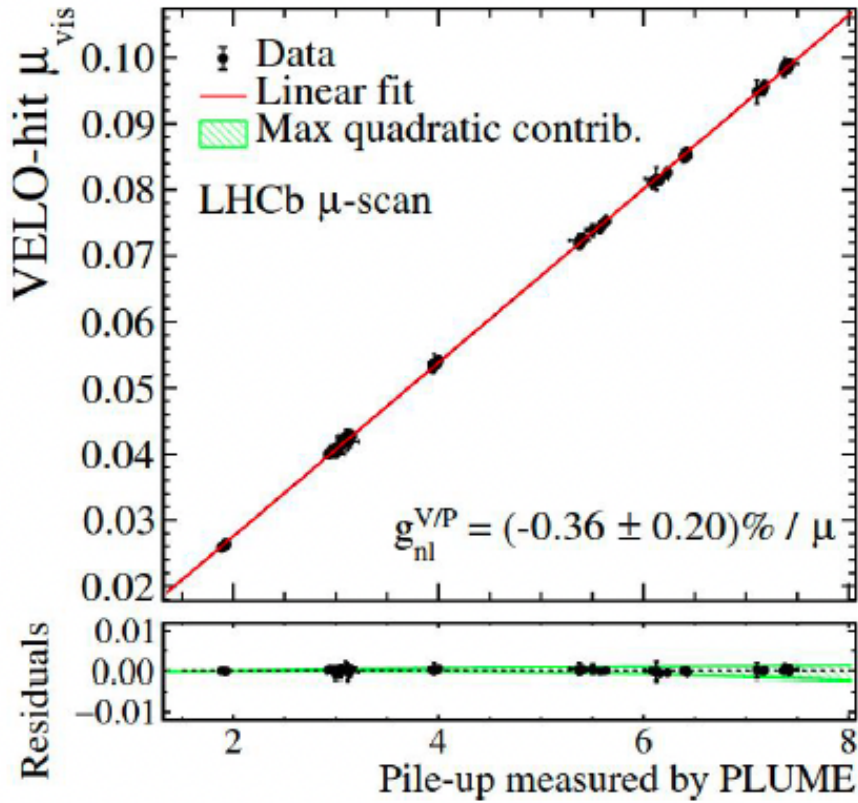


Figure 18: VELO-hit based linearity performance.

across the detector, the method can extract beam displacements in x , y , and z using a Principal Component Analysis (PCA)-based weighting. Preliminary studies during dedicated scans have demonstrated a beam spot resolution of approximately

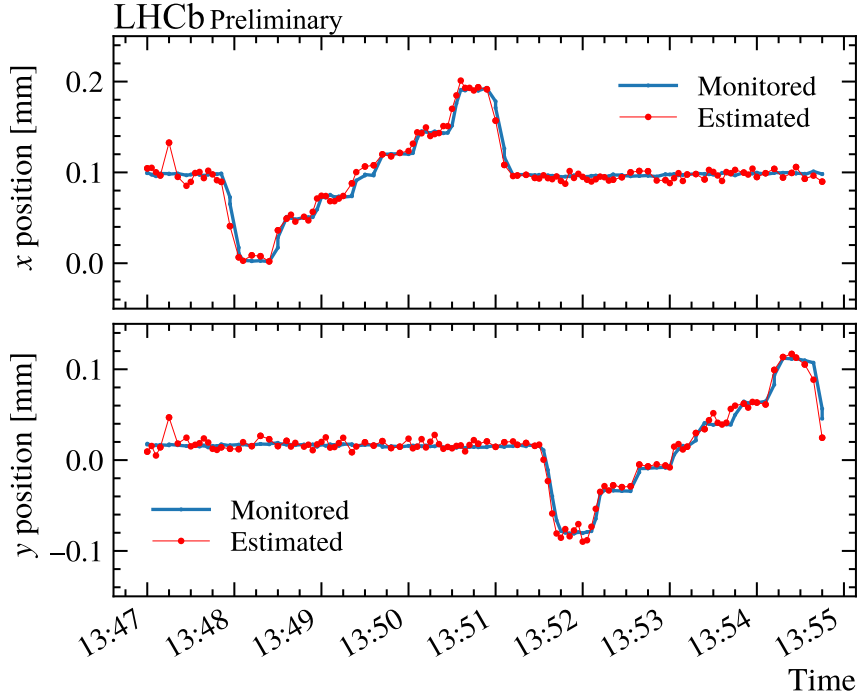


Figure 19: Trending plot of the x and y estimators (red), overlaid to the transverse beamline position provided by the VELO monitoring tasks (blue). The time period corresponds to a second LSC scan performed during Fill 9475 [April, 6th 2024], 30 minutes after the one used for calibration

4 μm every 3 seconds and a good agreement with the VELO-track estimator as shown in Fig. 19.

11.1 Offline luminosity determination

The data flow for the offline luminosity deployment has been finalised. A first version of the 2024 offline pp luminosity at $\sqrt{s} = 13.6$ TeV has been made available to analysts. For the total 2024 pp luminosity at $\sqrt{s} = 13.6$ TeV, 4612 runs have been processed. The ROOT files are produced by Analysis Production (AP), which processes the luminosity stream containing the LumiSummary, where the luminosity counters are stored at a rate of 30 kHz during physics data-taking. These files are then analysed to extract the visible number of interactions, μ_{vis} , for each colliding BXID in every run. This value, combined with the cross-section measured in the May 2024 vdM scan, allows for the measurement of the integrated luminosity per run. This procedure is repeated for every available counter. The released luminosity values are estimated using PLUME counters and the logZero method. Preliminary validation has been performed by comparing these values with luminosity measurements using VELO tracks and RICH hit counters, yielding agreements of $\sim 1\%$ and $\sim 2\%$, respectively. The offline luminosity values

are stored on an online server, accessible to analysts via the LumiCalib tool provided by the luminosity working group. Given an AP, this tool provides the offline luminosity per run and verifies dataset integrity by comparing the number of luminosity events propagated in the physics streams (via File Summary Records and stored in the analyst LumiTree) with the number of luminosity events in the luminosity stream used to compute the actual luminosity. The counting is consistent at the 0.1% level, with a negligible number of runs showing discrepancies of up to 20%. Since, at this stage, the bare cross-section from the vdM scan is used and main systematic corrections are missing in the vdM analysis, a preliminary 6% uncertainty is assigned to the offline luminosity. However, this uncertainty is expected to be reduced soon. In parallel with pp luminosity, the LumiCalib tool also provides the SMOG2 online luminosity, with a 10% error in runs where gas is injected. Regarding the 2025 data-taking plan, a preliminary program for vdM and emittance scans has been prepared. An early emittance scan is planned at the start of the 2025 data-taking, and the usual full pp vdM programme is expected, as in 2024. Additionally, an extended emittance scan has been planned for the p -O data-taking.

12 Real time analysis

The Upgrade trigger [6] is fully implemented in software. Collisions are reconstructed in real time with the best possible quality; candidates and event-level information are then selected and written to offline storage. This process is done in two steps. In the first one, HLT1, a fast reconstruction sequence is run on about 500 GP-GPUs to reduce the rate to about 1 MHz. Data are then stored in a disk buffer, enabling detector calibrations and derivation of alignment constants. Once ready, the second step, HLT2, performs the full reconstruction using CPUs on about 4000 nodes and either selects full events or individual particle candidates to be analysed further offline. In this scheme, the full reconstruction is performed online and not redone later.

12.1 First trigger stage

The first trigger stage (HLT1) has been in production since the first collisions at all instantaneous luminosities in 2024. During the first two weeks of October 2024 the system was run at nominal luminosity conditions and with the full set of tracking algorithms enabled. In November 2024 HLT1 has run for the heavy-ion data taking by employing a minimum bias strategy and a veto on high multiplicities.

During the YETS the effort focused on improving the robustness of the system and enhancing the performance in view of a stable luminosity production for the 2025 data taking. The VELO track pattern recognition was updated to mitigate possible efficiency losses due to missing modules. The pattern recognition involving the UT detector was improved to be more efficient, and the track reconstruction

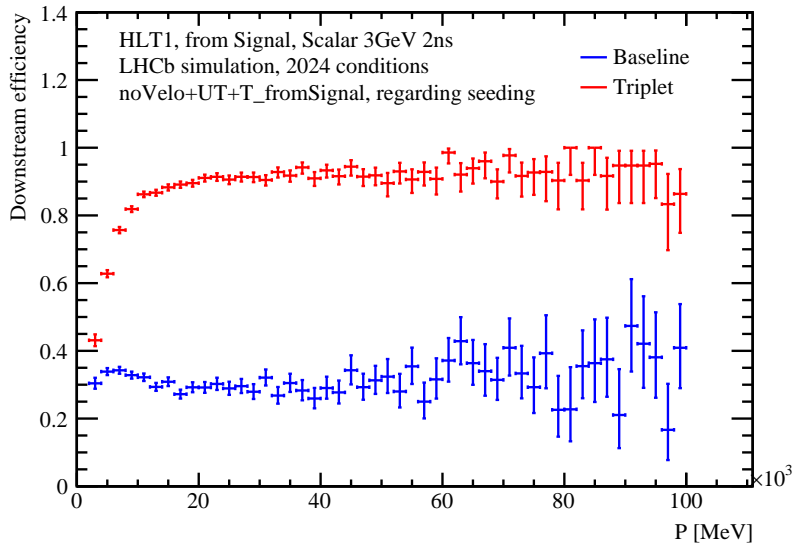


Figure 20: Comparison in reconstruction efficiency of long-living particles with a mass of $3 \text{ GeV}/c^2$, (blue) for the track reconstruction used in 2024 data taking and (red) the updated version for 2025 data taking, determined using simulation.

for long-lived particles was updated to increase the efficiency for (potential) heavy long-lived particles, as shown in Fig. 20 with a $3 \text{ GeV}/c^2$ particle as an example.

The track fit of particles traversing the full detector has also been improved by moving from a Kalman Filter employed only for the VELO segment, to a Kalman Filter using all subdetectors, which increases the accuracy of the state estimates, helps in reducing the ghost contribution and is expected to improve the number of signal decays per given bandwidth.

A series of studies have been conducted to assess the throughput of the system, due to the aforementioned changes and the removal of VELO shims (see 8.1). Furthermore a new so-called bandwidth division is being prepared. This serves the purpose of maximizing the total physics output of HLT1 by allocating a certain amount of output bandwidth for each HLT1 line and balancing this allocation with respect to all other HLT1 lines.

12.2 Alignment and calibration

The work done since the start of the YETS aimed at understanding and improving the alignment and calibration of the detector using the data collected during 2024 in view of the 2025 data taking. A major focus was on the online automatization procedure of the tracker alignment and on the π^0 calibration. At the beginning of March a campaign of magnetic field measurements was conducted in order to produce a more accurate field map able to reduce the dependence on the momentum scaling.

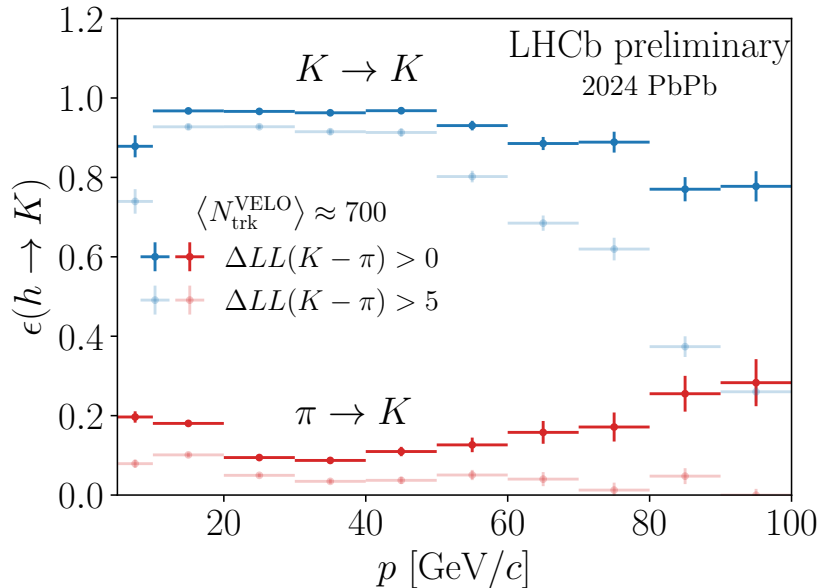


Figure 21: Kaon identification efficiency and pion misidentification probability as a function of momentum in lead-lead collisions. The average number of VELO tracks is 700 [LHCb-FIGURE-2025-05].

Thanks to the huge amount of 2024 calibration data, the tracking and particle identification performance could be studied in detail also with SMOG and lead-lead samples, using the tag-and-probe technique. The high quality performance of the RICH detectors, studied first in pp collisions with high purity $D^* \rightarrow D^0(K^- \pi^+) \pi^+$ decays, has been confirmed with the lead-lead data set. Figure 21 shows the kaon identification efficiency and pion misidentification probability as a function of momentum.

12.3 Second trigger stage

During the heavy-ion data taking period, HLT2 was reconstructing the full event with a global event cut of about 30'000 SciFi clusters and running with two physics streams: One stream saving candidates and all reconstructed objects, and one stream saving all detector raw banks in addition. This allows to perform the selection offline, and if needed, also to reconstruct (parts of) the event offline for more complex hadronic events. The processing of all events in HLT2 finished soon after the end of the 2024 data taking.

The main work carried out during the YETS concerned the consolidation of the reconstruction, and the optimization of the HLT2 output bandwidth to meet the tape and disk requirements.

There are two main improvements for the HLT2 track reconstruction in view

of 2025. The first concerns decays of long-lived particles, where the track finding now mitigates the lower efficiency of the UT detector for finding track segments. This leads to an overall increase in efficiency for decays of *e.g.* K_S^0 mesons that decay outside the detector volume of the VELO detector. The second is a significantly higher efficiency for low-momentum tracks that are bent out of the detector volume in the magnetic field and only leave charged clusters in the VELO and the UT trackers. The higher efficiency leads to an improved sensitivity for searches for light objects, such as dark photons decay to dielectron final states. Other improvements include a better efficiency for the reconstruction of neutral objects in the calorimeter due to a more robust (less occupancy dependent) matching between charged particle tracks and calorimeter clusters and a mechanism to store numerical information instead of reconstructed objects for isolation purposes.

Significant work went into maximizing the use of the available HLT2 output bandwidth. Apart from the optimisation of the selection criteria mostly carried out by the physics working groups, more fine-grained persistency options were employed to only save the necessary information, additional to the signal candidates, in the TURBO stream. The monitoring functionalities of the bandwidth tests were enhanced to give users a better judgement of the purity of their selection lines. In addition to the lines under the control of the physics working groups, the calibrations lines were optimized as well, adapting their rate and selection criteria to more closely reflect the need of the precision for analyses.

13 Online

The Online project has performed very well throughout 2024. Operational efficiency has been increased by improved automation. The capacity of the HLT2 event filter farm has been almost doubled by a refurbishment campaign, where several thousand old CPUs were replaced by newer models, which were acquired at low cost on the second-hand market. This was performed rolling in the background without impacting the system performance during LHC running. New storage has also been added. The low-level readout firmware and software has been improved with several releases, which fixed some minor issues and increased robustness. The March 2025 release is expected to be the last one for Run3. For the rest of Run3 on the hardware side, only maintenance is planned, and the software emphasis will be on increased robustness and modernization of older parts of the system.

Looking forward to LS3 and Run-4 we note a rather high rate of component failures among memory modules, spinning hard-drives and CPUs, in particular in the heavily used event-builder nodes. Although this is not a problem for Run-3, as there are many spares available, it is a clear sign that a part of the ageing online hardware infrastructure will need to be replaced for Run-4. A partial replacement of these nodes is being prepared and funds will be put aside from regular M&O funds for this replacement towards the end of LS3.

14 Electronics

There was progress on many fronts towards the LS3 enhancements. The FastRICH chip for the RICH enhancement was submitted for fabrication and will be delivered in May. Laboratory, irradiation and beam tests are being prepared. In parallel, FPGA firmware development started for data-transport in the PCIe40/PCIe400 frameworks. For the ECAL, a new design for power regulation of the front-end board (FEB) was prototyped and successfully tested with existing FEB. The first PCIe400 modules were assembled and are currently under test. The test programme is proceeding well and many features have already been verified. Finally, a market-survey was run jointly with CMS with the aim of identifying qualified vendors to replace obsolete low-voltage-power-supply components for Run-4.

Looking forward to Upgrade-II, work continued on new ASIC designs. A first version of the SPIDER ASIC for PicoCal was submitted for fabrication in February. Two more prototype ASICs (MightyPix2 for the Mighty-Tracker and ICECAL65 for PicoCal) passed design reviews and are targetting submission in early summer. Finally, the pixel part of the Mighty-Tracker underwent a major electronics-architecture review.

15 Software and computing

15.1 Data processing

LHCb data are further processed offline after the HLT2 trigger stage to prepare them for disk storage where it is made available to analysts. This processing is referred to as *Sprucing* and involves a combination of (depending on the HLT2 stream) data slimming, further data selections and a file reformat before being streamed to disk.

In 2024 LHCb spruced more than 35 PB of data concurrently with data-taking exploiting the WLCG resources in collaboration with the Computing team. For the FULL and TurCal streams the required 7.5x reduction in bandwidth between tape and disk was achieved.

There was an inherent data duplication in the streaming framework for TURBO data. Developments over the YETS have removed this data duplication reducing the required disk resources by around 30%. To retroactively recover 9PB of disk space, the TURBO stream of 2024 has been re-spruced in the first quarter of 2025. This was a significant operational undertaking for the DPA project, computing project and analysts; comprehensive validations were performed by analysts exploiting the CI infrastructure of analysis productions (see below). The foreseen re-sprucing of the FULL stream to allow for new selection lines to be run was successfully concluded for 2024 data during the YETS.

Analysis productions are a centralised way for analysts to create ntuples from the data stored on disk that again exploits the WLCG resources. The adoption

of analysis productions has been almost unanimous across Run 3 analyses. Developments on the analysis production platform now allow analysts to prescale the input data giving a mechanism for analysis prototyping on smaller datasets. The disk resources taken by analysis productions is now displayed by physics working group and by individual analysis with users encouraged via direct email to mark obsolete datasets as such (defined as those datasets that have not been accessed recently) so that they can be removed. Analysis productions can create a high I/O load on WLCG sites. To mitigate this, the streams out of the Sprucing (the input to analysis productions) are now further split into high and low rate lines. This was applied also to the TURBO data of 2024 when it was re-spruced to remove the data duplication.

To create nTuples, analysis productions run the DaVinci application which shares the same framework as the trigger and the Sprucing. It is the final application in the central data-processing chain. The memory consumption of running large DaVinci jobs can be problematic and progress has been made on reducing this; the DaVinci memory consumption is now monitored via performance tests which will facilitate further optimisation including multi-threading.

Ultimately, LHCb aims to allow for full dataset processing and filtering — including calibration routines and evaluation and cuts on derived quantities — using analysis productions exploiting the trivially parallelizable nature of these jobs and the WLCG resources.

The offline operations detailed above are the remit of the LHCb Data Processing and Analysis (DPA) project. Alongside this, the DPA project is responsible for the further exploitation of legacy Run 1 and 2 data, analysis preservation, open data and training within LHCb. The training work package has now delivered the Run 3 LHCb starterKit; the Run-1 and Run-2 version of which was instrumental in efficient on-boarding of new collaboration members.

15.2 Simulation

The simulation software continues to support productions for legacy datasets (Run 1 and Run 2), current datasets as they arrive (2024-2025) and future datasets (2025-2026, Run 4 and Run 5). In the last six months, efforts have been mostly focused on supporting both Run 3 data taking and whilst ensuring that Run-5 (LHCb Upgrade-II) simulation samples will be available for the sub-detector TDRs later this year.

Special attention continues to be paid to the simulated samples for 2024 data-taking, which are delivered in eight blocks with varying detector and trigger configurations. A focus of recent work is to prepare a significant update of the sub-detectors during each of the blocks, *e.g.* including/disabling sensors or modules in each block and improving the accuracy of the hit efficiencies in the digitisation step. This was deployed (`fill in`) and provides an excellent baseline for the first 2025 simulated samples, with expected conditions similar to those from the end of the 2024 *pp* run.

Over the last six months several simulation productions have been setup for the expected conditions of the heavy ion and pp reference runs in time for data-taking at the end of 2024. The productions representing the actual data taking conditions are deployed for the heavy ion samples are close to being available for the pp reference run too.

Work towards switching to the DD4hep detector description continues to be a priority, focusing on getting it production ready for use with both Run 3 and Run 5 detector geometries. For Run 5, bi-weekly meetings follow the progress of sub-detectors who have now delivered default material descriptions, allowing for a recent first release of the Run 5 geometry. The Run-3 subdetectors regularly provide feedback and improvements, many based on the data taken during 2024. Productions for Run 5 using Sim 11 are anticipated soon for the tracking detectors and by the end of the year for Run 3.

The Gauss(-on-Gaussino) software is now compiled and tested on the ARM architecture. First comparisons with standard CPU samples revealed a few discrepancies related to variables of type `char`, these have all now been fixed. Run 5 samples including the tracking system are good first candidates to be produced on opportunistic ARM resources.

Progress in exploiting fast simulation approaches has continued both in using possible machine learning models for the calorimeter response and using a point library approach. Studies are well advanced in each case, with the internal code review process in an advanced state for both approaches. Commissioning for production to allow for test usage by selected physics analysts will be the focus of the next six months.

15.3 Offline computing

The Offline computing team has been focusing its activities on the support for 2024 data taking and data productions. The efforts ensured that the data recorded in the pp and Heavy Ion runs were safely written to tape, distributed across across the Grid sites, spruced and made available for analysis in a timely manner. Production of Monte Carlo samples on the Grid also proceeded correctly. During the YETS, several re-sprucing and re-streaming campaigns were conducted, to produce data samples of increased quality, and reduced output size, for the benefit of the physics analyses.

The smooth operation of the distributed computing infrastructure, and the advancement of a fraction of the 2025 Tier-0 and Tier-1 storage resources, played a crucial role in these successful campaigns. A new Tier-2 site at Lanzhou University (China) providing CPU and disk resources was added to the LHCb Grid, and the NIKHEF Tier-2 site (in the Netherlands) have started to offer disk resources as well. A migration of the GGUS Grid Helpdesk affecting our support infrastructure took place in January 2025.

Good progress was made in the development of DIRACx, the major upgrade of the Data and Workload Management application used to manage the LHCb ac-

tivities. An initial version was released in March, and an update of the production infrastructure was deployed in early April.

The validation of the LHCb Monte Carlo stack on ARM processors is expected to finish soon, and work is already underway to include ARM clusters from sites such as Glasgow and CERN in the DIRAC production configuration.

Dedicated documents to present the final requests for the computing resources in 2026 [51], and the usage of computing resources in 2024 [52] have been submitted to the C-RSG.

16 Infrastructure

The YETS gave LHCb the opportunity to perform interventions on the detector, the infrastructure, and the detector services. The interventions were driven by the aim to improve the data quality and the data taking stability.

On the detector side the 0.5 mm shims of the VELO were successfully removed, and a resulting improvement of 10% in IP resolution is expected. A huge cleaning campaign of the SciFi VTRx optical links was performed to mitigate the effect of the outgassing. Not only the broken links were recovered but the preventive cleaning is expected to mitigate the consequences of the VTRx outgassing during the rest of run 3. More details on the detector work performed during the YETS can be found in their respective sections.

A campaign to improve the accuracy of the magnetic field map was performed. The goal was to expand the measurements beyond the central region by measuring outer planes of imaginary rectangle inside Magnet. The data are being analysed.

Civil Engineering Works have been carried in the UGC1 gallery to allow safe storage of ECAL modules during LS3. The connection of the low-temperature detector cooling systems to an uninterruptible power source, with backup from the Point-8 diesel generator in order to improve the resilience of the experiment against power outages, is still ongoing.

The replacement of the refrigeration coolant of the Main Chiller from R449a to R448a minimised the effects of oil accumulation in the heat exchangers of the MAUVE cooling plants and extended the acceptable operation time of the SciFi cooling plant (although the issue has not been fully resolved). The additional heat exchanger flushing system has a limited impact over time and is less effective than a complete system warm-up. Therefore, further modifications are under consideration, such as the addition of a new heat exchanger or the installation of an alternative filtering system (*e.g.*, activated carbon). The installation is affected by vibrations, which provoke the creation of unexpected leaks. The small heat exchangers of Tandem 2 will be reinstalled on a new supporting structure to better isolate them from the compressors' mechanical vibrations, serving as a preliminary test for a potential full modification during LS3. The Main Chiller backup mode was partially tested (Tandem 3 connected instead of Tandem 2), demonstrating the possibility of supporting three cooling systems using only two Tandems.

The C6F14 coolant in the SciFi cooling system was removed and replaced with approved NOVEC 7100, reducing the GWP to 297.

To increase MAUVE systems availability, a new CO₂ pump was purchased to ensure a high-availability spare unit for both MAUVE systems. Due to an increased hydraulic oil leak rate (about 1 L/month), the VELO CO₂ pump was dismantled and replaced with a spare unit, allowing the affected pump to be sent to the supplier for further inspection and maintenance. The Back Pressure Regulators were equipped with prototype flushing boxes to prevent condensation and freezing of water, which could potentially block the valves and disturb operation. Additional pipe extensions and spare pressure sensors were installed to increase the reliability and redundancy of the regulation equipment. Following the manufacturer’s recommendation, PLC communication cards were replaced along with new CAT6a cables to ensure stable communication across systems.

During the 2024 run, unusual weather conditions resulted in difficulties maintaining sufficient cooling parameters for magnet operation. In response to this issue, and in addition to the usual yearly maintenance, the heat exchangers were preventively inspected and cleaned to improve system efficiency. Further investigation is ongoing to propose new mitigation measures or potential system upgrades.

A new RICH1 gas recovery system has been constructed and is currently in the installation and commissioning phase. It is designed to enable RICH1 gas regeneration to operate simultaneously with the normal process. Previously, the old system could only regenerate gas when the main process was stopped.

A new ATEX-compliant gas mixing system was constructed and successfully installed to supply the new gas-based detector chamber located in the LHCb underground area. This system is part of the preparations for the detector’s commissioning, scheduled for 2025.

17 Upgrade-II status

A second major upgrade of the LHCb detector is necessary to maximise the physics potential of the HL-LHC. It will be installed after the completion of Run-4, by when the current detector will have accumulated its design integrated luminosity of 50 fb⁻¹. As shown in the LHCb Upgrade-II Framework Technical Design Report (FTDR) [16], by equipping subdetectors to provide fast timing information and using radiation-hard technologies, it will be possible to operate at instantaneous luminosity of up to $1.5 \times 10^{34} \text{ cm}^{-2} \text{ s}^{-1}$ while maintaining or even exceeding the detector performance in the current experiment. This will enable a total sample exceeding 300 fb⁻¹ to be integrated by the end of HL-LHC operation, and will give unprecedented sensitivity to physics beyond the Standard Model in beauty and charm physics. LHCb Upgrade-II will additionally provide several other unique science opportunities, including in hadron spectroscopy, in electroweak precision measurements, in dark sector searches and in studies of heavy ion collisions. The European Strategy for Particle Physics [53] vision of full exploitation of the High

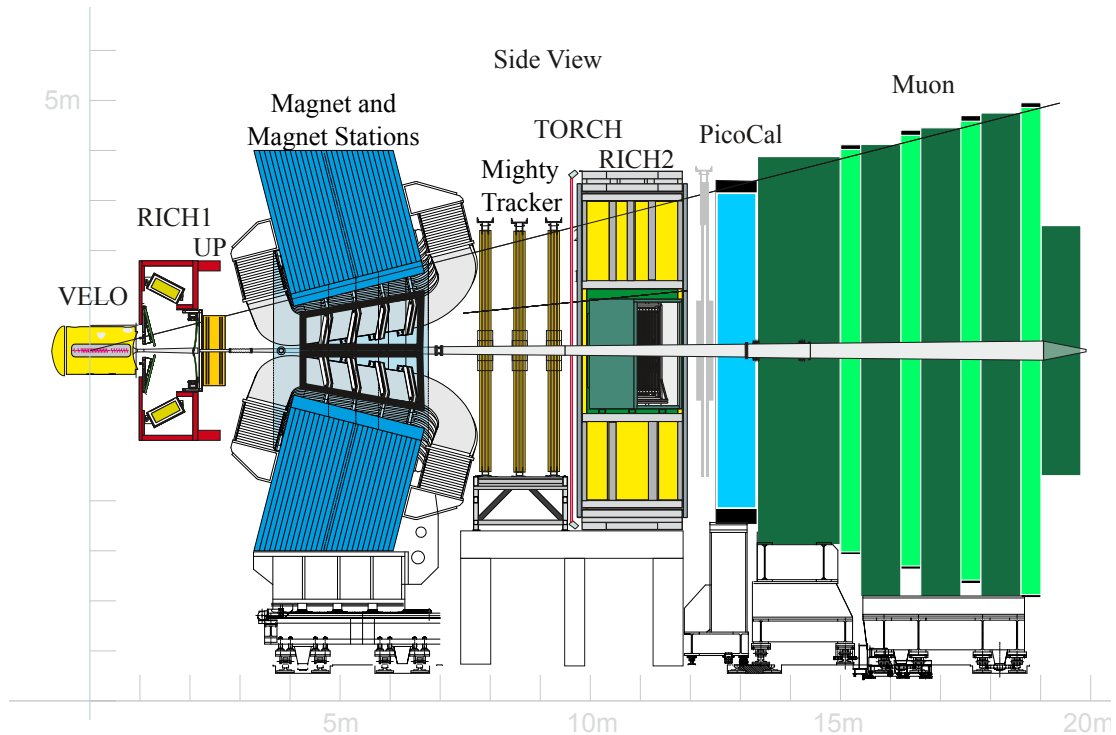


Figure 22: Schematic side-view of the Upgrade II baseline detector.

Luminosity LHC (HL-LHC), including flavour physics, can only be achieved with LHCb Upgrade-II.

A multi-step process to scrutinise and approve the Upgrade II project and secure the needed funding has been established by the LHCC [54]. To complete the first step of the process, a Scoping Document [55] has been prepared to complement the FTDR by adding information on detector scoping options matched to the established cost ranges of approximately 100%, 85% and 70% of the baseline cost outlined in the FTDR. The Scoping Document contains information on the financial envelope and physics performance in each of the descoped detector scenarios, on person-power and funding profiles, and on project organisation and milestones. The complete Scoping Document has been submitted to the LHCC for review on 2nd September 2024, as per the agreed schedule. The LHCC review consisted of detailed discussions at several meetings, including dedicated review meetings, with extensive written questions sent and responded to, with further iteration where needed. The review was concluded with the final version of the Scoping Document being made publicly available on CDS on 17th March 2025. A summary of the LHCC review was received by the CERN Research Board on 19th March 2025. The minutes of that meeting have not yet been published, but in draft form they state “The Research Board recommends that LHCb concentrates on the Middle scoping scenario,” noting that “the Middle scenario also appears to be well adapted to the expected resources.”

A schematic side-view of the Upgrade II detector is shown in Fig. 22. All

detector elements are retained in the Middle scenario. The main differences, with respect to the Baseline scenario, are

- Reduction of the the peak luminosity from 1.5 to $1.0 \times 10^{34} \text{ cm}^{-2} \text{ s}^{-1}$.
- Due to the reduced peak luminosity, the requirements on detector granularity are less stringent. The area covered by silicon pixels in the Mighty Tracker is reduced, from 2.1 m^2 to 1.3 m^2 per plane. Both the Muon and RICH detectors also have reduced granularity, and the active area of the TORCH detector is reduced.
- For the same reason of reduced peak luminosity, significantly less investment is required in the trigger farm.
- These detector simplifications lead to reduction of the total core capital cost, from $\sim 182 \text{ MCHF}$ to $\sim 156 \text{ MCHF}$.
- Due to the longer levelling time at lower peak luminosity, the reduction in total LHCb integrated luminosity is proportionately less than that of the peak value, but is still significant at $\sim 12\%$ (or $\sim 20\%$ with flat optics). This results in a loss in physics performance, as smaller data samples result in less precision on key observables, but the impact is relatively modest and a unique and compelling physics programme can still be achieved.

The LHCC have also recommended that two expert reviews, on the installation schedule and ASIC production for the ALICE and LHCb upgrades, should be set up. The CERN Research Board has endorsed this recommendation, noting that these should proceed in parallel with detailed discussions with the funding agencies to agree on the envelope of resources for the upgrade. The LHCb collaboration is fully ready to engage with these reviews as soon as they are set up.

The Scoping Document sets out plans for the project organisation and schedule. This includes preparation of Technical Design Reports (TDRs) for the sub-detectors by 2026, after which the project will move to the construction phase. Specifically, a TDR on the VELO is anticipated to be submitted for LHCC review in Q4/2026, a separate TDR on the remaining tracking detectors (UP, Mighty Tracker and Magnet Stations) should be submitted in Q3/2026, and a TDR on the particle identification detectors (RICH, TORCH, PicoCal, Muon) is planned to be submitted in Q2/2026. The use of common TDRs is intended to help ensure the coherence of the overall project, and also to facilitate the review. The TDRs will nonetheless contain, for each subdetector, detailed designs for the entirety of the system together with firm costs and schedules. In addition, a document will be produced to support the physical subdetector TDRs with common information about data processing, which will also contain details on the RTA and Online project schedules and management plans. The collaboration is now focussing its efforts to the preparation of these TDRs, with detailed planning of the tasks necessary in order to have all the required information by the relevant dates.

The completion of the reviews of the TDRs is the end of the second step of the multi-step scrutiny and approval process [54], after which it is anticipated that Memoranda of Understanding for LHCb Upgrade-II will be prepared.

LHCb has also actively engaged with the European Strategy for Particle Physics Update 2024–26, and has submitted a number of documents as part of the process. These are “Discovery potential of LHCb Upgrade-II” [56], “Technology developments for LHCb Upgrade-II” [57], “Heavy ion physics at LHCb Upgrade II” [58], “Computing and software for LHCb Upgrade-II” [59] and “Projections for key measurements in heavy flavour physics” [60]. The last of these was prepared together with the ATLAS, CMS and Belle II collaborations, and summarises and compares the expected sensitivities that can be achieved for a number of key observables in heavy flavour physics from the different experiments. This confirms that LHCb Upgrade II covers the broadest range of key observables, to which it has unsurpassed sensitivity, thus further underlining the uniqueness of its physics case.

References

- [1] LHCb collaboration, *Letter of Intent for the LHCb Upgrade*, CERN-LHCC-2011-001. LHCC-I-018, 2011.
- [2] LHCb collaboration, *Framework TDR for the LHCb Upgrade: Technical Design Report*, CERN-LHCC-2012-007, 2012.
- [3] LHCb collaboration, *LHCb VELO Upgrade Technical Design Report*, CERN-LHCC-2013-021, 2013.
- [4] LHCb collaboration, *LHCb PID Upgrade Technical Design Report*, CERN-LHCC-2013-022, 2013.
- [5] LHCb collaboration, *LHCb Tracker Upgrade Technical Design Report*, CERN-LHCC-2014-001, 2014.
- [6] LHCb collaboration, *LHCb Trigger and Online Upgrade Technical Design Report*, CERN-LHCC-2014-016, 2014.
- [7] LHCb collaboration, *LHCb Upgrade Software and Computing*, CERN-LHCC-2018-007, 2018.
- [8] LHCb collaboration, *Computing Model of the Upgrade LHCb experiment*, CERN-LHCC-2018-014, 2018.
- [9] LHCb collaboration, *LHCb SMOG Upgrade*, CERN-LHCC-2019-005, 2019.
- [10] LHCb collaboration, *LHCb Upgrade GPU High Level Trigger Technical Design Report*, CERN-LHCC-2020-006, 2020.

- [11] LHCb collaboration, *LHCb PLUME: Probe for Luminosity Measurement*, CERN-LHCC-2021-002, 2021.
- [12] LHCb collaboration, *Addendum No. 1 to the Memorandum of Understanding for Collaboration in the Construction of the LHCb Detector. The Upgrade of the LHCb Detector: Common Project items* CERN-RRB-2012-119A, revised April 2014, CERN, Geneva, 2012.
- [13] LHCb collaboration, *Addendum No. 2 to the Memorandum of Understanding for Collaboration in the Construction of the LHCb Detector Upgrade of the LHCb detector Sub-Detector Systems*, CERN-RRB-2014-105, 2014.
- [14] LHCb collaboration, *Expression of Interest for a Phase-II LHCb Upgrade: Opportunities in flavour physics, and beyond, in the HL-LHC era*, CERN-LHCC-2017-003, 2017.
- [15] LHCb collaboration, *Physics case for an LHCb Upgrade II — Opportunities in flavour physics, and beyond, in the HL-LHC era*, arXiv:1808.08865.
- [16] LHCb collaboration, *LHCb Framework TDR for the LHCb Upgrade II Opportunities in flavour physics, and beyond, in the HL-LHC era*, CERN-LHCC-2021-012, 2022.
- [17] LHCb Collaboration, *Computing model of the Upgrade LHCb experiment*, CERN-LHCC-2018-014. LHCb-TDR-018, CERN, Geneva, 2018.
- [18] LHCb collaboration, R. Aaij *et al.*, *Test of lepton flavour universality with $B_s^0 \rightarrow \phi \ell^+ \ell^-$ decays*, Phys. Rev. Lett. **134** (2025) 121803, arXiv:2410.13748.
- [19] LHCb collaboration, R. Aaij *et al.*, *Measurements of $\psi(2S)$ and $\chi_{c1}(3872)$ within fully reconstructed jets*, arXiv:2410.18018, Submitted to Eur. Phys. J. C.
- [20] LHCb collaboration, R. Aaij *et al.*, *Measurement of the CKM angle γ in $B^\pm \rightarrow DK^*(892)^\pm$ decays*, JHEP **02** (2025) 113, arXiv:2410.21115.
- [21] LHCb collaboration, R. Aaij *et al.*, *Study of $D_{s1}(2460)^+ \rightarrow D_s^+ \pi^+ \pi^-$ in $B \rightarrow \bar{D}^{(*)} D_s^+ \pi^+ \pi^-$ decays*, arXiv:2411.03399, Submitted to Science Bulletin.
- [22] LHCb collaboration, R. Aaij *et al.*, *Measurement of $\psi(2S)$ to J/ψ cross-section ratio as a function of centrality in PbPb collisions at $\sqrt{s_{NN}} = 5.02$ TeV*, arXiv:2411.05669, Submitted to JHEP.
- [23] LHCb collaboration, R. Aaij *et al.*, *Constraints on the photon polarisation in $b \rightarrow s\gamma$ transitions using $B_s^0 \rightarrow \phi e^+ e^-$ decays*, JHEP **03** (2025) 047, arXiv:2411.10219.

- [24] LHCb collaboration, R. Aaij *et al.*, *Measurement of ϕ meson production in fixed-target pNe collisions at $\sqrt{s_{NN}} = 68.5$ GeV at LHCb*, JHEP **03** (2025) 151, [arXiv:2411.09343](#).
- [25] LHCb collaboration, R. Aaij *et al.*, *First evidence for direct CP violation in beauty to charmonium decays*, Phys. Rev. Lett. **134** (2025) 101801, [arXiv:2411.12178](#).
- [26] LHCb collaboration, R. Aaij *et al.*, *Study of Λ_b^0 and Ξ_b^0 decays to $\Lambda h^+ h'^-$ and evidence for CP violation in $\Lambda_b^0 \rightarrow \Lambda K^+ K^-$* , Phys. Rev. Lett. **134** (2025) 101802, [arXiv:2411.15441](#).
- [27] LHCb collaboration, R. Aaij *et al.*, *Observation of the open-charm tetraquark state $T_{cs0}^*(2870)^0$ in the $B^- \rightarrow D^- D^0 K_S^0$ decay*, Phys. Rev. Lett. **134** (2025) 101901, [arXiv:2411.19781](#).
- [28] LHCb collaboration, R. Aaij *et al.*, *Search for D^0 meson decays to $\pi^+ \pi^- e^+ e^-$ and $K^+ K^- e^+ e^-$ final states*, [arXiv:2412.09414](#), Submitted to Phys. Rev. Lett.
- [29] LHCb collaboration, R. Aaij *et al.*, *Test of lepton flavour universality with $B^+ \rightarrow K^+ \pi^+ \pi^- \ell^+ \ell^-$ decays*, [arXiv:2412.11645](#), Submitted to Phys. Rev. Lett.
- [30] LHCb collaboration, R. Aaij *et al.*, *Measurement of CP asymmetries in $\Lambda_b^0 \rightarrow p h^-$ decays*, [arXiv:2412.13958](#), Submitted to Phys. Rev. D.
- [31] LHCb collaboration, R. Aaij *et al.*, *Measurement of CP asymmetry in $B_s^0 \rightarrow D_s^\mp K^\pm$ decays*, JHEP **03** (2025) 139, [arXiv:2412.14074](#).
- [32] LHCb collaboration, R. Aaij *et al.*, *Study of light meson resonances decaying to $K_S^0 K \pi$ in the $B \rightarrow (K_S^0 K \pi) K$ channels*, [arXiv:2501.06483](#), Submitted to Phys. Rev. D.
- [33] LHCb collaboration, R. Aaij *et al.*, *Search for charge-parity violation in semileptonically tagged $D^0 \rightarrow K^+ \pi^-$ decays*, JHEP **03** (2025) 149, [arXiv:2501.11635](#).
- [34] LHCb collaboration, R. Aaij *et al.*, *Observation of the $\Lambda_b^0 \rightarrow J/\psi \Xi^- K^+$ and $\Xi_b^0 \rightarrow J/\psi \Xi^- \pi^+$ decays*, [arXiv:2501.12779](#), Submitted to Eur. Phys. J. C.
- [35] LHCb collaboration, R. Aaij *et al.*, *Measurement of the $B^- \rightarrow D^{*0} \tau^- \bar{\nu}_\tau$ decay rate*, LHCb-PAPER-2024-037, in preparation, to be submitted to Phys. Rev. Lett.
- [36] LHCb collaboration, R. Aaij *et al.*, *Measurement of the multiplicity dependence of Υ production ratios in pp collisions at $\sqrt{s} = 13$ TeV*, [arXiv:2501.12611](#), Submitted to JHEP.

- [37] LHCb collaboration, R. Aaij *et al.*, *Search for resonance-enhanced CP and angular asymmetries in the $\Lambda_c^+ \rightarrow p\mu^+\mu^-$ decay at LHCb*, arXiv:2502.04013, Submitted to Phys. Rev. D.
- [38] LHCb collaboration, R. Aaij *et al.*, *Angular analysis of $B^0 \rightarrow K^{*0}e^+e^-$ decays*, arXiv:2502.10291, Submitted to JHEP.
- [39] LHCb collaboration, R. Aaij *et al.*, *Observation of a new charmed baryon decaying to $\Xi_c^+\pi^+\pi^-$* , arXiv:2502.18987, Submitted to Phys. Rev. Lett.
- [40] LHCb collaboration, R. Aaij *et al.*, *Branching fraction measurement of the decay $B^+ \rightarrow \psi(2S)\phi(1020)K^+$* , arXiv:2503.02711, Submitted to Phys. Rev. D.
- [41] LHCb collaboration, R. Aaij *et al.*, *Observation of charge-parity symmetry breaking in baryon decays*, arXiv:2503.16954, submitted to Nature.
- [42] LHCb collaboration, R. Aaij *et al.*, *Observation of the doubly-charmed-baryon decay $\Xi_{cc}^{++} \rightarrow \Xi_c^0\pi^+\pi^+$* , arXiv:2504.05063, submitted to JHEP.
- [43] LHCb collaboration, R. Aaij *et al.*, *Observation of the very rare $\Sigma^+ \rightarrow p\mu^+\mu^-$ decay*, arXiv:2504.06096, submitted to Phys. Rev. Lett.
- [44] LHCb collaboration, R. Aaij *et al.*, *Angular analysis of the decay $B_s^0 \rightarrow \phi e^+e^-$* , arXiv:2504.06346, submitted to JHEP.
- [45] LHCb collaboration, R. Aaij *et al.*, *Observations of $\Lambda_b^0 \rightarrow \Lambda K^+\pi^-$ and $\Lambda_b^0 \rightarrow \Lambda K^+K^-$ decays and searches for other Λ_b^0 and Ξ_b^0 decays to Λh^+h^- final states*, JHEP **05** (2016) 081, arXiv:1603.00413.
- [46] LHCb collaboration, *Simultaneous determination of the CKM angle γ and parameters related to mixing and CP violation in the charm sector*, LHCb-CONF-2024-004, 2024.
- [47] O. B. Garcia *et al.*, *High-density gas target at the lhc experiment*, Physical Review Accelerators and Beams **27** (2024) .
- [48] LHCb collaboration, *RICH Performance Plots - Cherenkov Angle Resolutions for RICH 1 and RICH 2*, LHCb-FIGURE-2023-007, 2023.
- [49] LHCb collaboration, *Hadron PID Performance in 2024*, LHCb-FIGURE-2024-031 (2024).
- [50] RICH collaboration, P. A. Cartelle *et al.*, *Luminosity measurement with the LHCb RICH detectors in Run 3*, submitted to JINST (2025) arXiv:2503.05273.
- [51] C. Bozzi *et al.*, *LHCb Computing Resources: 2026 requests*, CERN, Geneva, 2025.

- [52] C. Bozzi, *LHCb Computing Resource usage in 2024* , CERN, Geneva, 2025.
- [53] European Strategy Group, *Deliberation document on the 2020 update of the European Strategy for Particle Physics*, CERN-ESU-014, 2020.
- [54] Large Hadron Collider Committee, *LHC Experiments Phase IIb Upgrades Approval Process*, CERN-LHCC-2022-012, 2022.
- [55] LHCb collaboration, *LHCb Upgrade II Scoping Document*, CERN-LHCC-2024-010, 2025.
- [56] LHCb collaboration, *Discovery potential of LHCb Upgrade II*, LHCb-PUB-2025-001, 2025.
- [57] LHCb collaboration, *Technology developments for LHCb Upgrade II*, LHCb-PUB-2025-002, 2025.
- [58] LHCb collaboration, *Heavy ion physics with LHCb Upgrade II*, LHCb-PUB-2025-003, 2025.
- [59] LHCb collaboration, *Computing and software for LHCb Upgrade II*, LHCb-PUB-2025-004, 2025.
- [60] ATLAS, Belle II, CMS and LHCb collaborations, *Projections for Key Measurements in Heavy Flavour Physics*, LHCb-PUB-2025-008, 2025.